Mesoscale Temperature and Moisture Fields from Satellite Infrared Soundings

By
Donald W. Hillger and Thomas H. Vonder Haar

Department of Atmospheric Science
Colorado State University
Fort Collins, Colorado

May 1976

Colorado State University

Department of Atmospheric Science

Paper No. 249

MESOSCALE TEMPERATURE AND MOISTURE FIELDS
FROM SATELLITE INFRARED SOUNDINGS

by

Donald W. Hillger

and

Thomas H. Vonder Haar

Department of Atmospheric Science

Colorado State University

Fort Collins, Colorado 80523

May 1976

AUTHOR'S NOTE

The text of this paper was originally the thesis presented
in partial fulfillment of the requirements of the Degree of Master
of Science for Donald W. Hillger, April 1976, entitled: "Mesoscale
Temperature and Moisture Fields from VTPR Sounding Radiances".
The slight change in title is due to the applicability of the methods
presented herein to satellite infrared sounders other than the VTPR.
The results of this paper will also be presented at the COSPAR Symposium
on Meteorological Observations from Space, in June 1976. A condensed
version will subsequently be published in the symposium proceedings.

ABSTRACT

The combined use of radiosonde and satellite infrared soundings can provide mesoscale temperature and moisture fields at the time of satellite coverage. Radiance data from the Vertical Temperature Profile Radiometer (VTPR) on NOAA polar-orbiting satellites can be used along with a radiosonde sounding as an initial guess in an iterative retrieval algorithm. The mesoscale temperature and moisture fields at local 9 - 10 a.m., which are produced by retrieving temperature profiles at each scan spot for the VTPR (every 70 km), can be used for analysis or as a forecasting tool for subsequent weather events during the day.

By using radiosonde and satellite soundings in a combined mode we have a product which is better than either system alone. The advantage of better horizontal resolution of satellite soundings can be coupled with the radiosonde temperature and moisture profile both as a best initial guess profile and as a means of eliminating problems due to the limited vertical resolution of satellite soundings.

The combined data coverage and resolution equals or surpasses interpolation between existing radiosonde stations. Even with only one available radiosonde sounding, the mesoscale temperature and moisture structure around the radiosonde can be deduced. When several such mesoscale fields are combined the resultant high resolution synoptic field is compared to conventional analyses using radiosondes alone.

ACKNOWLEDGEMENTS

TABLE OF CONTENTS

LIST OF TABLES

LIST OF FIGURES

1.0 INTRODUCTION

The advent of passive vertical temperature soundings from satellites has provided a new tool for the atmospheric scientist. Previous to the development of remote soundings the only means of probing the vertical structure of the atmosphere was by use of radiosonde balloons or rocketsondes. These instruments actually sensed the surrounding atmosphere through which they passed. However, the satellite thermal sounder is a passive instrument which senses infrared radiances in several wavelength intervals as seen from the satellite.

These radiances are signatures of the thermal structure of the atmosphere in a vertical column below the sounder. The radiative transfer equation provides the physics which connects the temperature structure to the radiances as seen at the top of the atmosphere. The problem is then one of "inverting" the equation of radiative transfer to retrieve the thermal structure of the atmosphere which produced the observed radiances. There is no unique solution to this retrieval problem; however, solutions do exist which provide relatively accurate determinations of the atmospheric temperature profile. One major problem in the retrieval technique involves the case of cloudy atmosphere where both cloud height and amount must be determined before the effect of the clouds can be accounted for and an accurate temperature profile can be retrieved. However, even a very simple cloud correction technique which determines an effective cloud top height alone can be useful in retrieving temperature profiles above this effective cloud top level, thereby eliminating many problems caused by low level clouds.

Once the retrieval of the temperature profile is accomplished, we have available a powerful tool which is revolutionizing atmospheric sounding. At their present stage of development, satellite sounders are not about to replace conventional radiosondes, but they prove very useful as a supplement to the radiosonde. The radiosonde is designed to be both inexpensive and accurate, but to be used extensively without sacrificing accuracy it would be too expensive to be practical. This is where the satellite sounder has an application.

The satellite sounder can provide thermal soundings on a larger scale and with better horizontal resolution than possible with radiosondes alone. These facts, however, do not make the satellite sounder a superior instrument. Due to the limits of passive sounding theory the satellite sounder has restricted vertical resolution. Thus, the two instruments used in a combined mode can provide the vertical and horizontal resolution needed for many of the requirements of mesoscale research.

The main reason for the development of satellite sounders was to fill in data sparse regions over the oceans. Much research has shown the usefulness of satellite soundings in regions where radiosonde data is otherwise not available (Smith et. al., 1975; Dyck, 1975). However, this same data can also be useful on a smaller scale to fill in the gaps between the standard radiosonde stations. With radiosonde soundings alone, synoptic scale temperature analyses are drawn by interpolating between existing radiosonde stations. Interpolation is a technique which proves to be a true representation provided temperature gradients are linear and small scale temperature fluctuations or anomalies do not occur. If more detailed mesoscale information is desired

the answer may lie in satellite soundings. Even if only one radiosonde is launched the local mesoscale temperature and moisture structure may be deduced by the combined use of satellite and radiosonde soundings.

If satellite coverage is available, the additional satellite soundings can provide both the 3-dimensional thermal structure and 2-dimensional moisture structure around the radiosonde sounding. A time dimension is also available if the satellite soundings occur at a different time than the radiosonde sounding. True time dimension coverage will be available with the placement of remote sounders on geosynchronous satellites (Suomi et al., 1971). The Vertical Atmospheric Sounder (VAS) system, a second-generation sounder similar to the Vertical Temperature Profile Radiometer (VTPR) on NOAA polar-orbiting satellites, should be launched around 1978.

At the present time with sounders on polar-orbiting satellites the most easily realized advantage is that of horizontal spatial resolution far surpassing that of any operational radiosonde sounding network. This resolution for VTPR is about 70 km or on the order of every half degree of latitude and is available in the form of radiances. This is by no means a lower limit to passive sounding resolution and is being steadily improved with new technology. The most recent experimental sounder already in operation, the High Resolution Infrared Sounder (HIRS) on Nimbus-6, has a resolution of 25 km, more than double the resolution of VTPR, or roughly four soundings in every half-degree latitude-longitude square.

The use of the satellite soundings on this scale assumes that the soundings are readily obtainable by the user. Since the use of satellite soundings up to this time has been concerned mainly with data-

sparse regions the operational retrieval of temperature soundings was accomplished only over the oceans. If soundings are desired on a smaller scale or over land areas the temperature profiles must be produced by a program or algorithm designed to use the satellite data on the desired scale. If the data are stretched to the resolution limit by retrieving a temperature sounding at every scan spot then precautions must be taken to avoid random errors. Where less resolution is required the temperatures can be averaged to eliminate many of these random errors.

After briefly describing the theory of atmospheric sounding and the technique used to retrieve temperature soundings we will discuss some encouraging results of using VTPR on the mesoscale over land. These results show the usefulness of the increased data resolution on the mesoscale as well as the feasibility of applying this technique to many types of similar mesoscale problems.

2.0 THEORY OF REMOTE SOUNDINGS

The theory of sounding the vertical structure of the atmosphere using radiance measurements was first explained by Kaplan (1959). The idea is dependent upon an absorbing gas with constant mixing ratio, such as carbon dioxide (CO_2), in the atmosphere. At some wavelengths, such as 15 microns, the atmosphere is opaque to radiation even on a relatively small length scale such as the vertical depth of the atmosphere. The CO_2 absorption band around 15 microns, as shown in Figure 1, can then be utilized to vertically probe the atmospheric thermal structure. By looking in the wings of such an absorption band the atmospheric depth becomes less opaque for shorter or longer wavelengths. These less opaque channels will see deeper into the atmosphere and may be transparent enough to sense the surface radiance also. Much less opaque channels near 12 microns, such as in the atmospheric window region, sense the surface radiation almost entirely with very little atmospheric contribution.

The 15 micron CO_2 absorption band has been used widely for several reasons. Another CO_2 absorption band around 4.3 microns can be used as well but has some radiation characteristics which make 15 microns a better choice for present technology. Namely, the absolute energy emitted near 15 microns is several times larger than that emitted near 4.3 microns especially for the low 200+ Kelvin temperatures encountered in the upper troposphere. Another reason is the better temperature sensitivity relative to noise energy level of the 15 micron radiation at low temperatures. At these temperatures the absolute energy received at
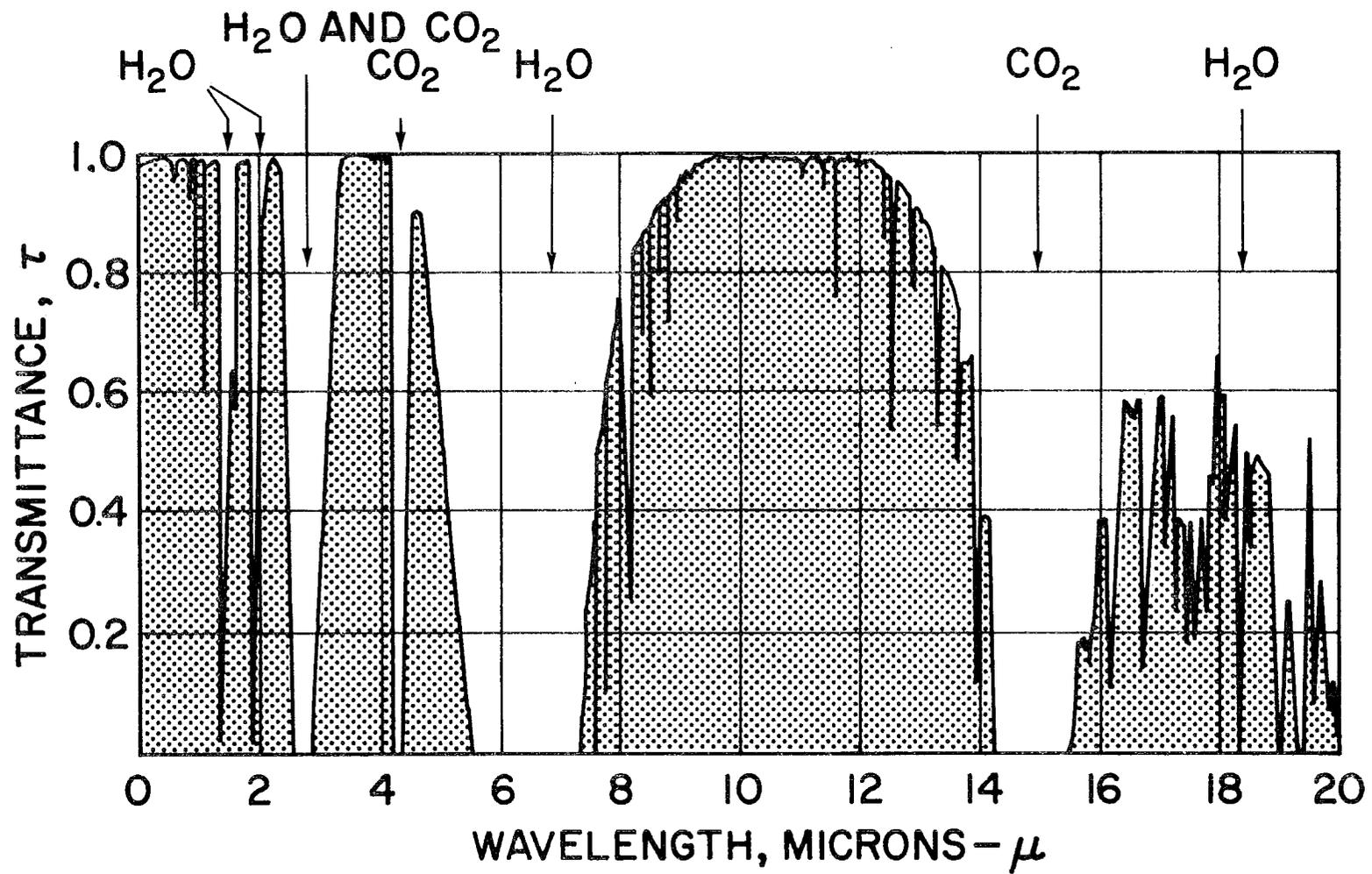
Figure 1. Infrared Transmission Spectrum (Hall, 1974)

4.3 microns is small compared to that at 15 microns although the change in relative radiance as a function of temperature is larger at 4.3 microns (Smith, 1972).

A couple of the first successful satellite sounding experiments, SIRS-A and B on Nimbus-3 and 4, used the 15 micron CO_2 absorption band. These first generation sounders paved the way for the present VTPR operational sounder which also uses the 15 micron band alone.

By utilizing radiance channels in the short wavelength wing of the 15 micron CO_2 absorption band, where water vapor absorption is less noticeable than in the long wavelength wing, radiance information can be used to infer the vertical temperature structure of the atmosphere. Each different radiance channel will sense the thermal structure from a different position in the vertical column of the atmosphere. The fact that these radiances are not independent makes the temperature retrieval problem non-unique.

3.0 RADIATIVE TRANSFER EQUATION

The radiative transfer equation in Table 1 governs the vertical radiation path from the surface of the earth to the satellite. The first term represents surface radiance which is sensed by the satellite if the transmission of the total atmospheric depth is non-zero for a given channel or wavelength interval. Some of the more opaque radiance channels with zero transmittance at the surface will not contain this surface contribution but only contributions from layers of the atmosphere above the surface.

From a series of such equations, one for each radiance channel, the inverse problem of radiative transfer, or solving the equations for the temperature or blackbody radiance profile of the atmosphere, may be accomplished (Wark and Fleming, 1966; Fritz et al., 1972). Three retrieval methods are listed in Table 2. It must be remembered that the solution is not always unique especially in cloudy cases since cloud amount and vertical distribution is not easily determined. For cloudy cases the infrared transmission below the clouds is zero but clouds may not cover the entire field of view. However, sufficient horizontal resolution may allow the satellite sounder to see between and therefore below the clouds. Clouds present a special problem which must be dealt with in any temperature retrieval technique. Once a retrieval algorithm is devised, cloudy columns can either be eliminated or an attempt can be made to account for the clouds, as was done in this study in the simplest form of an effective cloud top height above which soundings were available.

RADIATIVE TRANSFER EQUATION SYMBOLS

$$N_i(\nu_i) = B\left[\nu_i, T(p_0)\right] \tau\left[\nu_i, U(p_0)\right] \varepsilon$$

(surface term)

$$-\int_0^{P_0} B\left[\nu_i, T(p)\right] \frac{\partial \tau\left[\nu_i, U(p)\right]}{\partial p} dp$$

(atmospheric term)

negative sign due to transmittance decreasing with increasing pressure (looking down through the atmosphere from above $\partial \tau/\partial p$ is negative)

$i = 1, 2, \ldots m$ (m = number of channels, i.e. m = 8 for VTPR)

Symbol	Explanation

$N_i(\nu_i)$ = spectral radiance observed at the top of the atmosphere in a spectral interval $\Delta \nu$ around mean wavenumber ν_i

$B\left[\nu_i, T(p)\right] = \dfrac{c_1 \nu_i^3}{\exp\,(c_2 \nu_i/T(p))-1}$ (c_1, c_2 constants)

= Planck blackbody radiance at mean wavenumber ν_i and temperature $T(p)$ at pressure p.

$\tau\left[\nu_i, U(p)\right]$ = transmittance at mean wavenumber ν_i of the mass of optically active absorbing gas $U(p)$ above pressure p (i.e., CO_2 transmittance).

ε = surface emissivity. (assumed $\varepsilon = 1$.)

$\dfrac{\partial \tau\left[\nu_i, U(p)\right]}{\partial p}$ = derivative of transmittance function τ w.r.t. some function of pressure p (Planck radiance weighting functions for the radiative transfer equation).

dp = pressure increment for finite summations of the atmospheric term through the vertical depth of the atmosphere.

p_0 = surface pressure or effective cloud top pressure

Table 1.

TEMPERATURE RETRIEVAL METHODS

Definition:

Methods to solve the inverse problem of radiative transfer. (Methods for retrieving the temperature profile $T(p)$ as a function of the independent variable pressure p from a set of radiances N_i, one for each sounding channel at mean wavenumber ν_i)

Method	Explanation
Regression method	Regression equations derived from a dependent set of radiosonde measurements that are coincident in space and time with satellite radiance measurements to determine temperatures at specific levels.
Inverse matrix method (full statistics)	Solve a set of simultaneous equations one for each radiance channel using matrix manipulations.
Direct retrieval* (iterative method)	Iterative calculations of the radiances until the residual from the observed radiance is smaller than a predetermined "noise" value. (First guess temperature profile is adjusted to bring calculated radiances into closer agreement with the observed radiances - repeated until convergence occurs to a pre-set "noise" level for the radiances).

Table 2.

*Method used in this study

4.0 TRANSMISSION AND WEIGHTING FUNCTIONS

Since the mixing ratio of CO_2 in the atmosphere is almost constant, we can assume that changes in radiance as sensed by a satellite for a given CO_2 channel are due to atmospheric temperature and moisture changes alone. The transmission of the atmosphere due to CO_2 is also slightly dependent on temperature, but this is of lesser magnitude and can be accounted for with temperature-dependent CO_2 transmittances (Smith, 1969). The effect of varying amounts of water vapor on the transmission functions is of higher order than temperature effects, but other than these second order effects the transmittances are only dependent on the amount of CO_2 absorbing gas and on pressure which remain fairly constant.

The derivatives of the CO_2 transmittances with respect to some function of pressure give CO_2 weighting functions for the atmospheric contribution to the radiance sensed by the satellite. Examples of CO_2 transmittances and weighting functions for the U.S. standard atmosphere are shown in Figure 2 and 3.

The peak or maximum of these weighting functions represents the level from which the maximum radiance contribution in a given channel originates. Below this level more radiation is absorbed by layers between the source and the satellite, and above this level less absorbing and emitting gas with decreasing pressure causes less contribution to the total radiance.

To reconstruct the satellite-sensed radiances from a given temperature profile requires an integration through all the layers of the atmosphere of the radiance contribution from each layer modified by the weighting function for that layer. A temperature profile as shown in
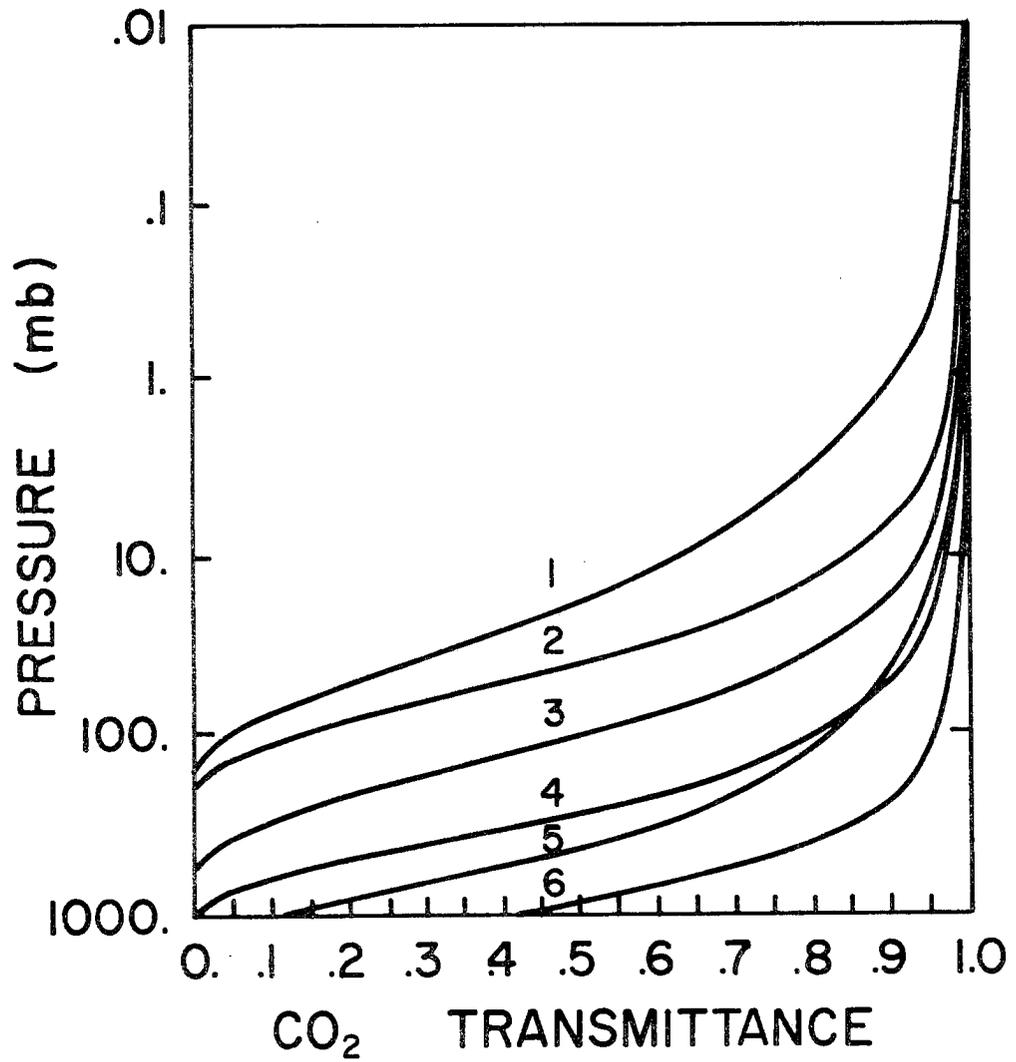
Figure 2.   VTPR CO_2 Channel Transmittances
for US Standard Atmosphere
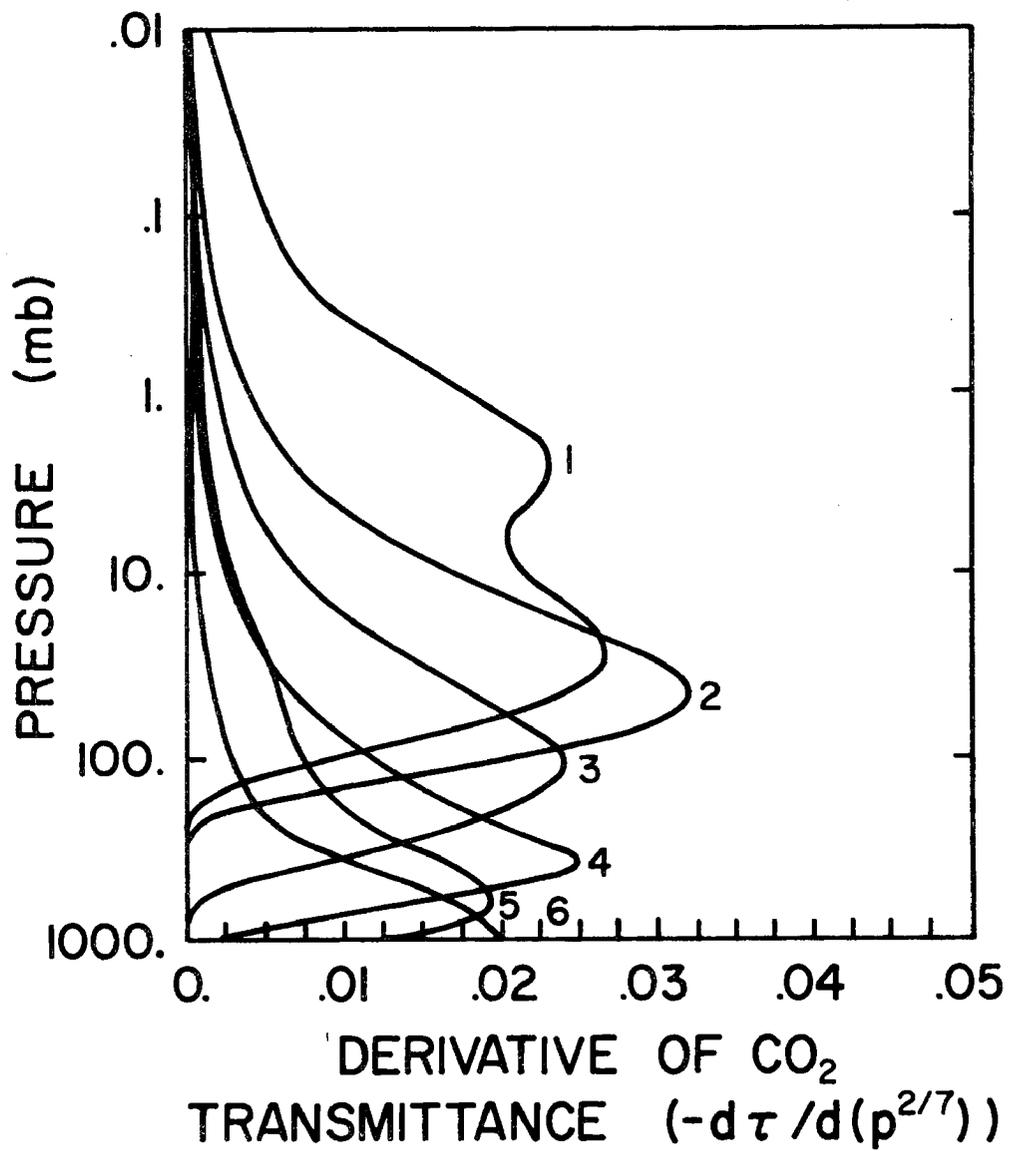
Figure 3. VTPR CO_2 Channel Weighting Functions for US Standard Atmosphere

Figure 4 will produce a blackbody radiance profile similar in shape to the given temperature profile. This blackbody radiance profile when multiplied by the weighting function for a radiance channel will produce a vertical profile of the actual radiance contribution for the given channel. These actual radiance contributions shown in Figure 5 look similar to the original weighting functions, but the peaks are shifted towards higher temperatures at the surface and stratopause. In this form the curves represent actual contributions to the radiative transfer equation, and the integral or area under these curves represents the integrated or total radiance sensed by the satellite for each channel.
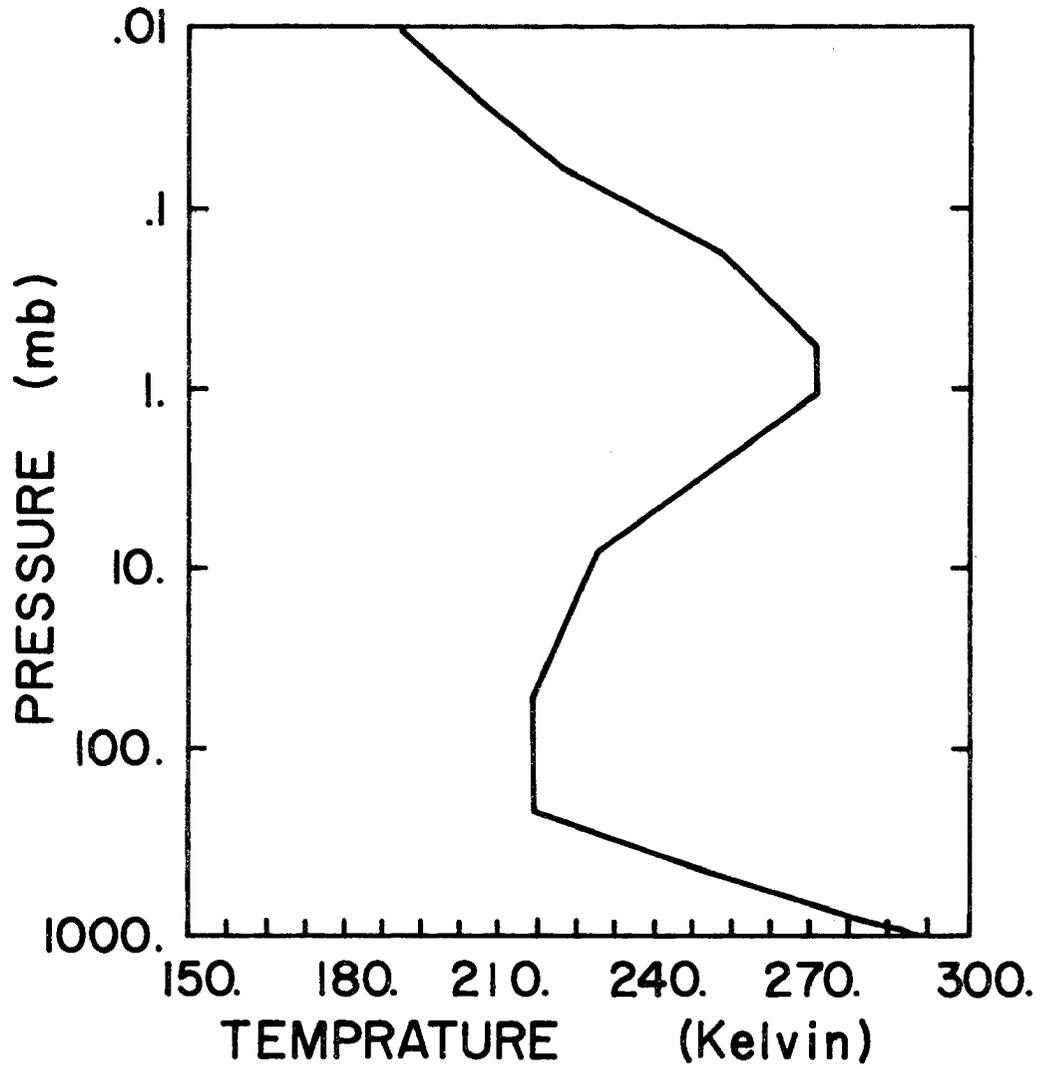
Figure 4. Standard Atmosphere Supplement
Mid-latitude Spring-Fall
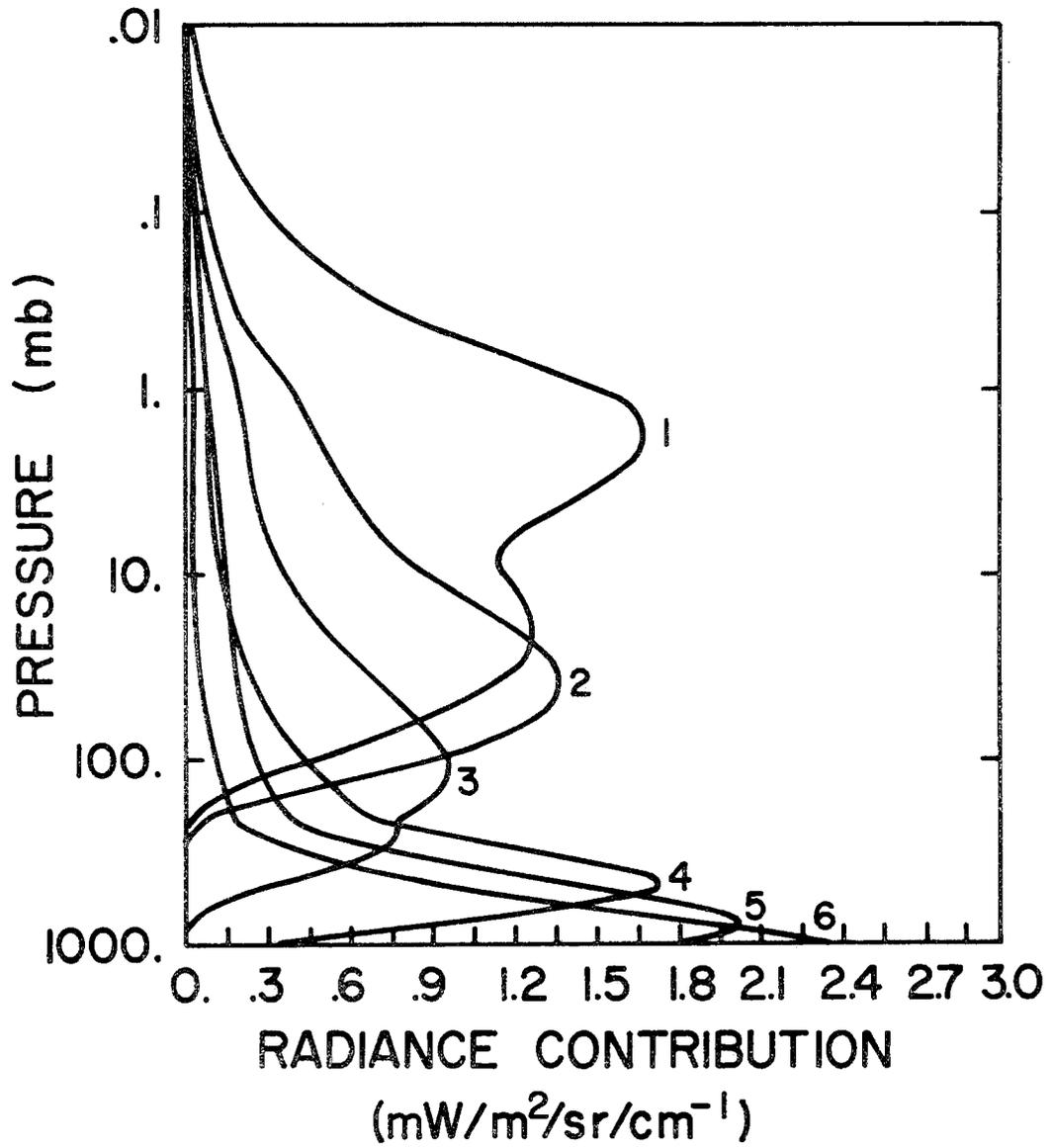
Figure 5. VTPR CO$_2$ Channel Radiance Contributions

5.0 PRESENT-DAY SATELLITE SOUNDERS

Two different second-generation vertical atmospheric sounders were launched in the early 1970's. The Vertical Temperature Profile Radiometer (VTPR) on board NOAA operational satellites has 6 CO_2 channels for temperature profiling, a water vapor absorption channel to get an idea of vertically integrated water vapor, and a window channel to sense surface or cloud top temperature. The other instrument, the Infrared Temperature Profile Radiometer (ITPR) on board the Nimbus-5 experimental satellite, is part of the Nimbus-5 Sounding System which also includes microwave channels to see through clouds. In the infrared spectrum, ITPR has 5 CO_2 channels, one water vapor channel, and two window channels. The channel wavenumbers and peak levels of weighting functions for VTPR and ITPR are listed in Tables 3 and 4. The weighting functions for the ITPR channels shown in Figure 6 are similar to those previously shown for the VTPR.

Data on satellite orbits, scan coverage and resolution are compared for the two sounders in Table 5. Both satellites have similar sun-synchronous orbits with twice daily coverage of the whole earth except for different local equator crossing times. On the issue of coverage and resolution: what ITPR gains in resolution (4 times area resolution of VTPR) it loses in coverage (1/3 area coverage of VTPR). See Figures 7 and 8 for displays of scan patterns for VTPR and ITPR. The fact that ITPR lacks continuous surface coverage is a hinderance in this study. Since temperature soundings are retrieved over land areas from ITPR radiances and not VTPR, ITPR can be more desirable in some applications. However, this problem was overcome by the development of a temperature retrieval program to use radiances at every scan spot for the NOAA VTPR.

NOAA VTPR CHANNELS

CHANNEL NUMBER	WAVELENGTH (microns)	WAVENUMBER (cm^{-1})	APPROXIMATE PEAK LEVEL OF WEIGHTING FUNCTION (millibars)
CO_2 channels: (15 micron CO_2 absorption band)			
1 (Q branch)	14.96	668.5	30
2	14.77	677.5	50
3	14.38	695.0	120
4	14.12	708.0	400
5	13.79	725.0	600
6	13.38	747.0	surface
H_2O channel: (Rotational water vapor absorption band)			
7	18.69	535.0	600
Window channel: (Atmospheric window region)			
8	11.97	833.0	surface

Table 3.

NIMBUS-5 ITPR CHANNELS

CHANNEL NUMBER	WAVELENGTH (microns)	WAVENUMBER (cm^{-1})	APPROXIMATE PEAK LEVEL OF WEIGHTING FUNCTION (millibars)
CO_2 channels: (15 micron CO_2 absorption band)			
6 (Q branch)	14.96	668.3	30
5	14.50	689.5	120
4	14.01	713.8	500
3	13.39	747.0	surface
H_2O channel: (Rotational water vapor absorption band)			
7	19.71	507.3	700
Window channels: (Atmospheric window regions)			
1	3.73	2682.0	surface
2	11.12	899.0	surface

Table 4.
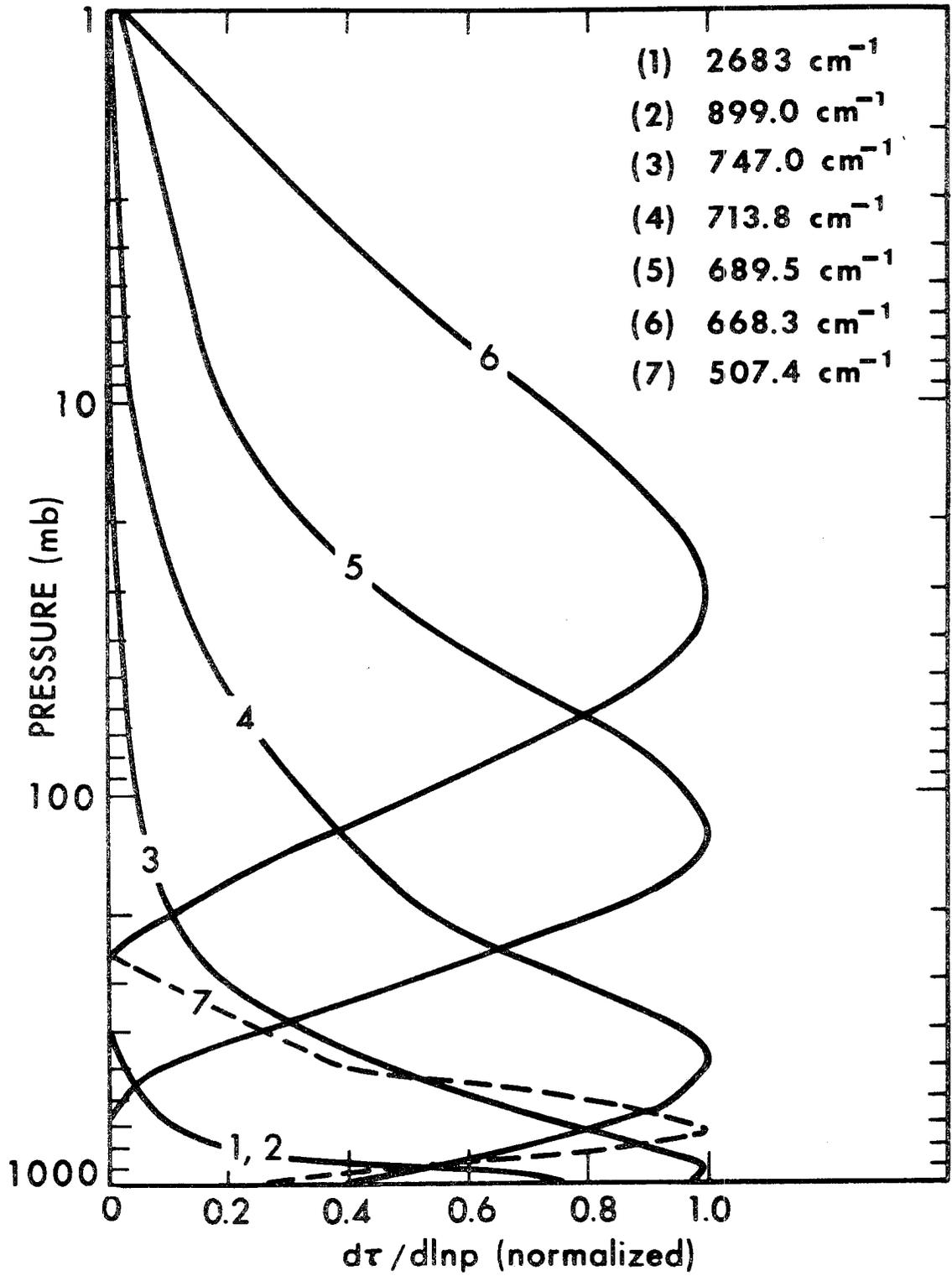
Figure 6.   ITPR Weighting Functions
(Nimbus-5 User's Guide)

COMPARATIVE SATELLITE SOUNDER CHARACTERISTICS

Sounder:	VTPR (Vertical Temperature Profile Radiometer)	ITPR* (Infrared Temperature Profile Radiometer)
Satellites:	NOAA-2,3,4 (operational)	Nimbus-5 (experimental)
Orbit:	78.3° retrograde sun-synchronous	81° retrograde sun-synchronous
Altitude:	1464 km	1112 km
Period:	115 minutes	107 minutes
Equator crossing: ascending descending	local 9 pm local 9 am	local noon local midnight
Maximum Scan Angle:	±30.3°	±35.1°
Coverage along satellite track:	Continuous scanning in 23 incremental spots/scan (12.5 sec/scan)	Intermittant in 3 scan-grid positions (left, center and right) of 10 scans of 14 spots/scan (approx. 1/3 area coverage of VTPR)
Spot size at NADIR:	67 km x 70 km (rectangular)	35 km (circular) (4 times area resolution of VTPR)
Soundings: standard procedure:	3 soundings each 8 scan lines of 23 spots (1 sounding every $(600 \text{ km})^2$) (operational soundings produced only over the data sparse oceans)	12 soundings in each scan-grid position (1 sounding every $(120 \text{ km})^2$)
resolution limit:	One sounding every scan spot $(70 \text{ km})^2$ over land or ocean	One sounding every scan spot $(35 \text{ km})^2$ over land or ocean.

Table 5.

*The Nimbus-5 Sounding System also includes the NEMS (Nimbus-E Microwave Spectrometer) and SCR (Selective Chopper Radiometer) instruments
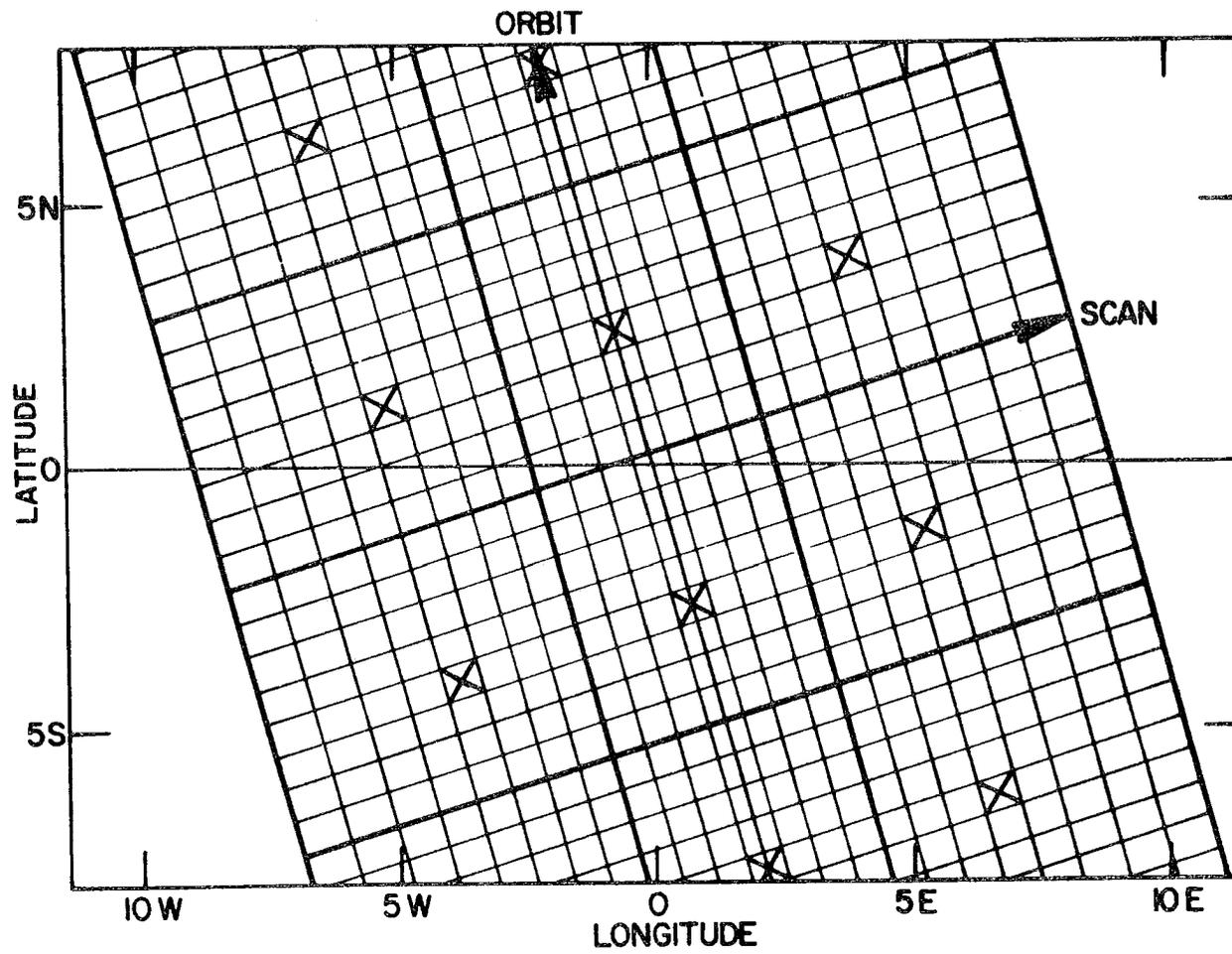
Figure 7. VTPR Scan Pattern (McMillin, 1973)
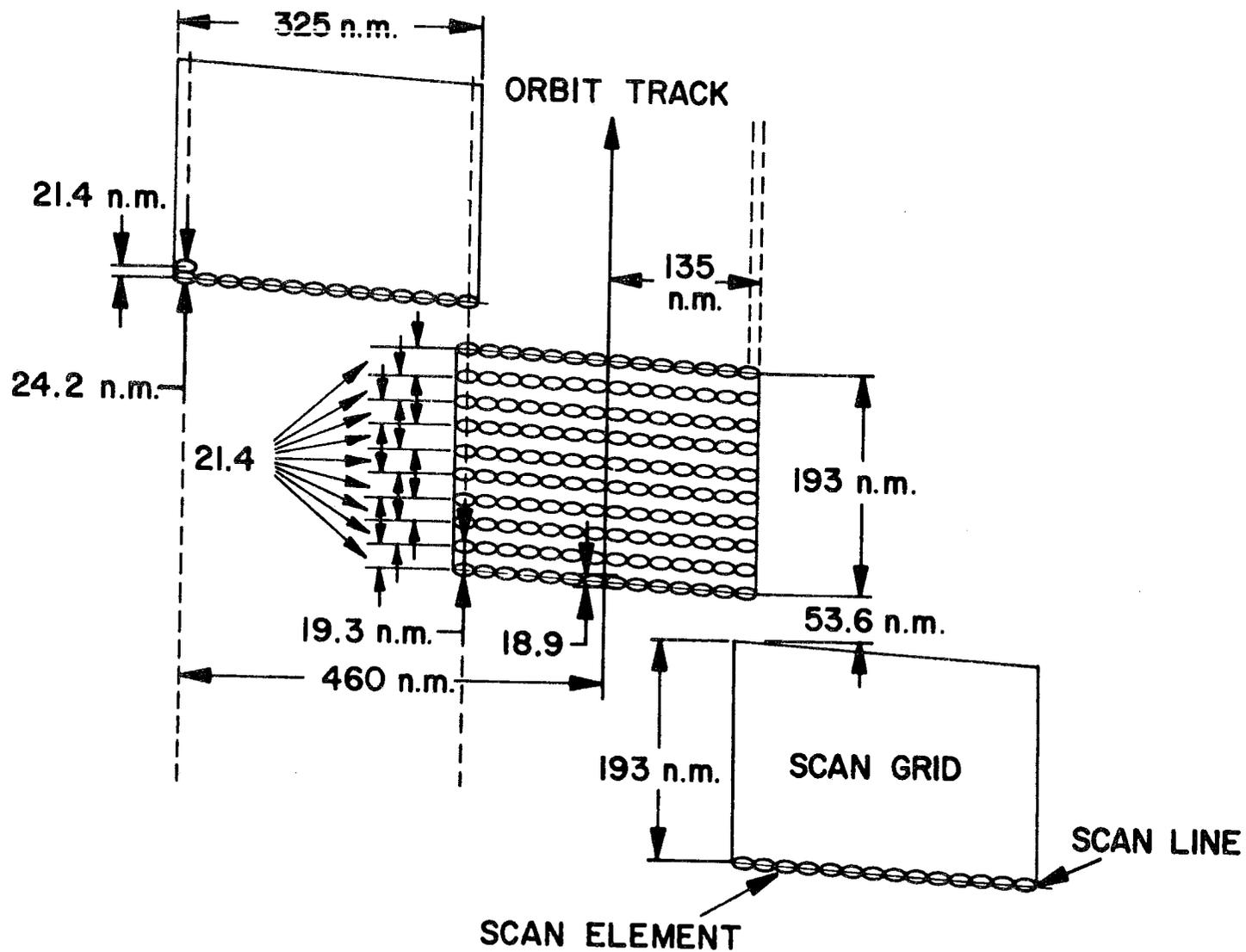
Figure 8. ITPR Scan-Grid Pattern (Nimbus-5 User's Guide)

6.0 COMBINED ANALYSIS OF SATELLITE AND RADIOSONDE SOUNDINGS

The idea of using satellite vertical temperature profiles along with conventional radiosonde soundings is to make use of the advantages of each system to gain the most from the combined data. The advantages and disadvantages of each system are listed for comparison in Table 6. Although the list is not complete, the most important considerations, such as resolution, are complimentary for the two systems. What satellite vertical temperature profiles lack in vertical resolution due to broad weighting functions, they gain in horizontal coverage and resolution, and whereas the radiosonde sounder has better vertical resolution, it lacks the horizontal resolution to fill in the details between standard radiosonde sites. Therefore, by combining these two data sources it is possible to better quantize the 3-dimensional nature of the atmosphere. The technique used is analagous to a "tree" with the radiosonde providing the "trunk and roots" or vertical resolution and surface pressure and temperature. The "branches" on this tree will be provided by the high-resolution temperature soundings derived from satellite radiances. The satellite sounder will therefore fill in the horizontal dimensions in the temperature and moisture fields around the radiosonde.

ADVANTAGES AND DISADVANTAGES OF SATELLITE
AND RADIOSONDE SOUNDINGS

	Satellite Soundings	Radiosonde Soundings
Resolution: -Spatial:	good horizontal resolution	good vertical resolution
	vertical resolution limited by broad weighting functions	poor horizontal resolution unless many coincident but closely spaced soundings are taken
-Time:	time resolution of 12 hrs on polar-orbiting satellites (soon every 30 minutes on geosynchronous satellites)	time resolution of 12 hrs (standard operational procedure) unless more frequent soundings are taken
Coverage:	global coverage of soundings even in remote or inaccessable areas such as over the oceans	soundings only where radiosondes are launched and tracked
Data Quality: -Temperature:	data best in the upper troposphere and stratosphere	data best in lower layers up to the tropopause or where the radiosonde stops transmitting
	multiple solutions of derived temperature profiles, for cloudy cases and the low levels.	instrument errors and data dropouts likely at high altitudes.
-Moisture:	only one value for the integrated moisture content of the atmosphere from one water vapor channel on present sounders (moisture profiles from several H_2O channels on new and future satellite sounders)	moisture profiles for the lower troposphere

Table 6.

7.0 TEMPERATURE RETRIEVAL PROGRAM FOR NOAA VTPR

The development of a temperature retrieval program was necessary to realize the horizontal resolution which satellite sounders are capable of producing. For the purposes of this task an iterative type program was chosen which could utilize a radiosonde sounding as the first guess in the iterative process. All iterative type retrieval algorithms produce better results when the initial guess temperature profile is more nearly like the temperature profile desired. Therefore, by using a radiosonde temperature profile which was taken at a time period near the satellite pass, the temperature field around the radiosonde sounding can be supplied with fairly good accuracy. In some cases climatological mean temperature profiles can be used as the initial guess profiles where no other better temperature profile or forecast profile is available. However, by utilizing an available radiosonde, the errors in the iterated temperature profiles can be reduced. The initial guess radiosonde sounding will be the closest match to the desired profiles with only slight changes to the initial guess. This is due to the basic persistent nature of the temperature structure of the atmosphere. All temperature changes produced will be due to changes in the satellite-sensed radiances, and when such changes are above noise level they are a result of changes in the actual thermal structure in space and time.

The iterative retrieval program used was modeled after a similar program developed by L. Duncan at the U.S. Army White Sands Missile Range (Duncan, 1974, a and b). This program uses an iterative relaxation formula devised by Chahine (1968 and 1970) to try to match calculated radiances to observed radiances through iterative changes in the initial

guess temperature profile. A schematic of the iterative retrieval algorithm is shown in Figure 9. After 25 iterations the temperature profile obtained is considered to be as close to that desired as is possible. Convergence may be obtained in less than 25 iterations if the residuals between the observed and calculated radiance for all 6 CO_2 channels are less than some pre-set "noise" level. This "noise" level was set at .25 $mW/m^2/sr/cm^{-1}$ (McMillin, 1973). Usually after 25 iterations this criterion is satisfied by all but possibly one or two channels, but if iterations were continued computational errors could magnify and excessive computer time would not produce better results. The convergence criterion and the number of iterations are two variables which account for some of the non-uniqueness of clear atmospheric soundings. The changes produced by these different criterion are usually less than $1^{o}C$ which is below the noise level of 1 to $2^{o}C$ (RMS) inherent in iterated temperature profiles due to random errors in the satellite radiances.

An example of initial and iterated temperature profiles is shown in Figure 10 to illustrate the type of profiles produced. Both the initial guess temperature profile and the final iterated temperature profile after 25 iterations are shown. Temperatures are derived at 100 pressure levels between .01 mb and 1000 mb, or fewer than 100 levels if the surface pressure is less than 1000 mb. Since temperatures are derived at many levels, 50 levels of which are between 100 mb and 1000 mb, it is possible to calculate the temperature at any level in the vertical. Certain standard levels can be used to illustrate the horizontal resolution and ability to detect horizontal temperature changes on the mesoscale.

ITERATIVE TEMPERATURE RETRIEVAL ALGORITHM
FOR VTPR CO_2 CHANNEL RADIANCES

(To produce a temperature profile T(p) by iteration
to match observed VTPR CO_2 channel radiances R_{obs} (1-6))

INPUT ————▶ Initial guess tempera- — — —▶ Transmittance and weight-
ture and moisture pro-
files $T_0(p)Q_0(p)$(i.e.
radiosonde sounding)
ing function calculations
for CO_2 channels 1-6

New temperature pro- ————▶ Integrated (calculated)
file T(p)
radiances using radiative
transfer equation (CO_2
channels 1-6)

Observed radiances ————▶ Equal or within a set
R_{obs} (1-6)(VTPR CO_2
channels 1-6)
noise level?

NO   YES

Modify temperature
profile T(p) by an it-
erative relaxation for-
mula (Chahine or Smith)
Temperature profile T(p)
is desired profile which
gives observed radiances
for CO_2 channels

OUTPUT

Note: During this process $Q_0(p)$ and the weighting functions for all
channels (1-8) remain the same.

Only the 6 CO_2 channels are actively used in the iterative
retrieval algorithm (the H_2O and window channels are used
only passively for comparison with observed radiances).
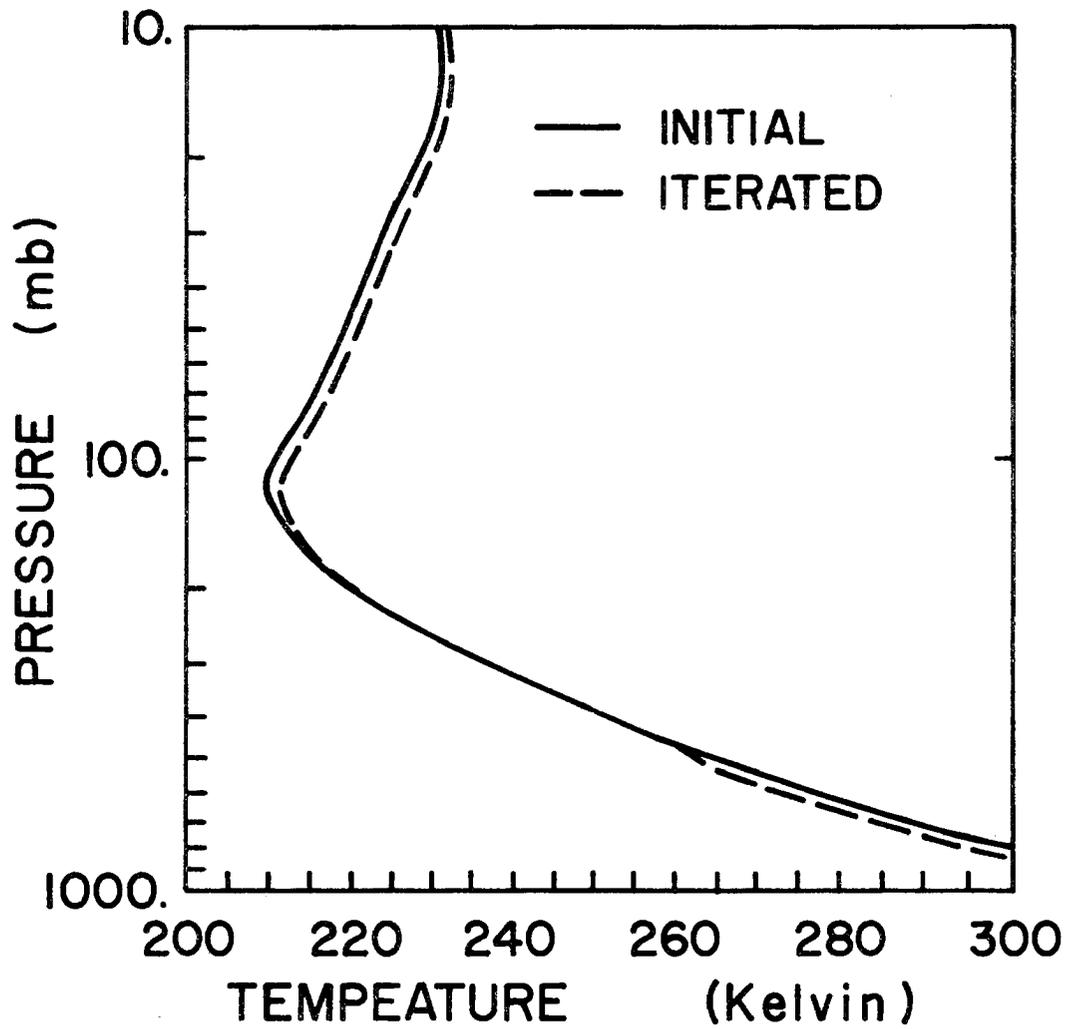
Figure 9.

Figure 10. Example -- Initial and Iterated Temperature
Profiles (Lander 7 August 1973 17 GMT)

The initial guess temperature profile is perturbed mainly at 6 levels where the weighting functions for the 6 CO_2 channels peak out, but the actual temperature at any level is a weighted combination of temperatures derived from all 6 channels. Perturbations to the initial guess temperature profile are on the order of 1^0 to 3^0C. If larger perturbations occur at levels other than near the surface when clouds are not present, this perturbation may appear as a bias error in all retrieved temperature soundings in the horizontal field. This type of bias is most common in the lower stratosphere or near the surface and may be due to a bias in the observed radiances, the initial guess profile, or in the transmittances used in the inversion program. Many of these biases can be readily detected by their large deviation from the initial guess radiosonde temperature profile, but because of time differences between the radiosonde sounding and the satellite pass this bias may or may not be real. Only with satellite and radiosonde soundings coincident in space and time can these biases be truly detected, but even if bias errors are present they would show up in all the derived temperature profiles in the mesoscale field and should not affect the magnitude of horizontal temperature changes which might appear.

The temperature retrieval program uses the initial guess radiosonde sounding for two main purposes as shown in Figure 11, besides as an initial guess profile. One use is to correct the CO_2 transmittances for temperature. These CO_2 transmittances are slightly temperature dependent, so the better the initial guess temperature profile, the better the transmittances used and the better the resultant temperature profiles produced. The other reason is to use the radiosonde moisture

TRANSMITTANCE AND WEIGHTING FUNCTION CALCULATIONS
FOR VTPR CHANNELS

Initial guess
temperature profile
$T_0(p)$

Initial guess
mixing ratio
profile $Q_0(p)$

Ozone transmit-
tances (mean
transmittances)

Modify CO_2 transmit-
tances for temperature
(Smith Polynomials)

Calculate H_2O
transmittances us-
ing $T_0(p)$ & $Q_0(p)$

Total transmittances
(channels 1-6)(pro-
duct of CO_2, O_3 and
H_2O transmittances)

Transmittances
(channels 7 & 8)
H_2O transmittances
only)

Weighting functions
(channels 1-6)(deriva-
tives of total trans-
mittances w.r.t. $p^{2/7}$)

Weighting functions
(channels 7 & 8)
(derivative of H_2O
transmittances
w.r.t. $p^{2/7}$)

CO_2 Channels. Used ac-
tively in iterative
temperature retieval
algorithm

H_2O and window chan-
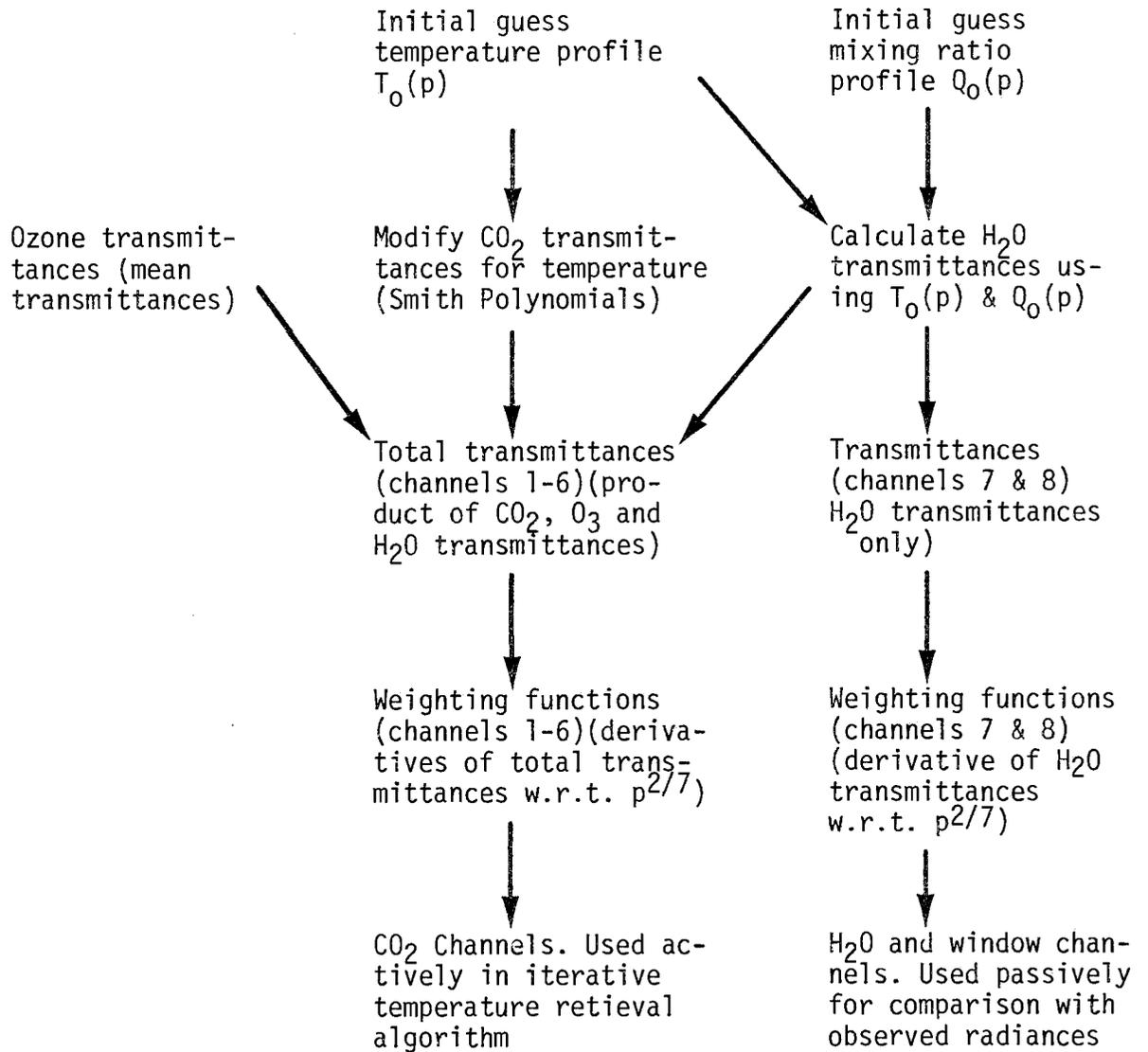nels. Used passively
for comparison with
observed radiances

Figure 11.

profile to calculate water vapor (H_2O) transmittances (Duncan, 1975). Once CO_2 and H_2O transmittances are calculated they are multiplied together along with mean ozone (O_3) transmittances to produce the total transmittances for the 6 CO_2 channels. These total transmittances are then used to calculate the weighting functions to the 6 CO_2 channels which are used actively in the temperature retrieval algorithm. This same set of transmittances, except for corrections due to different scan angles, is used to retrieve all the soundings in the mesoscale grid around the initial guess temperature profile.

Since only one water vapor channel is available in the VTPR sounding set we are unable to derive water vapor profiles for the mesoscale field around the initial guess radiosonde sounding. However, we can get an idea of the vertically integrated H_2O content using this channel (Wark, et al., 1974). By comparing the calculated radiance with the observed radiance in the H_2O channel we can determine if the integrated water content supplied by the initial guess radiosonde sounding is too small or too large. If more water vapor is actually present in a scan spot the observed radiance will be low due to a weighting function which peaks out at colder temperatures higher in the atmosphere. The higher calculated radiance will be an indication of initial guess moisture profile which is too dry or the presence of more water vapor in the observed vertical column. So, besides deriving mesoscale temperatures which can be used to determine stability, we can also achieve an indication of variations of the vertically integrated water vapor around the radiosonde.

8.0 MESOSCALE CASE STUDY DAYS

Two days, 7 and 9 August 1973 were chosen as case study days to use in this joint satellite-radiosonde study. NOAA-2 VTPR radiances were available at approximately 17 and 04 GMT (10 and 21 MST) on both days as listed in Table 7. Radiosonde soundings to use as initial guess profiles were available at the standard times of 12, 00, and 12 GMT the next day. (5, 17, and 5 MST).

The 17 GMT (10 MST) satellite radiances were chosen for study because of the possibility of determining mesoscale temperature and moisture fields which would be useful in forecasting convective development later in the day. Also, we have a choice of two available radiosonde soundings to use as initial guess profiles, one earlier and one later than the satellite pass. It seems the choice would be obviously the earlier radiosonde sounding at 12 GMT (night), however, the later sounding at 00 GMT (day) proved to be a better initial guess. In many cases, the earlier 12 GMT sounding contained a surface temperature inversion which would very likely not show up at the time of the satellite pass. When the earlier radiosonde soundings were used, the derived temperature profiles contained a surface temperature inversion similar to that of the initial guess radiosonde profile. For this reason the later 00 GMT radiosonde launch proved to be more satisfactory, considering that inversions are usually dissipated by 10 MST at this time of the year. It may be difficult in operational use to use a radiosonde sounding at a later time period but this problem can be alleviated by smoothing out the surface temperature inversion in the 12 GMT sounding if it is to be used as initial guess to retrieve temperature profiles at a time when an inversion is not expected. It would also help to know the surface

CASE STUDY DAYS

	NOAA-2 VTPR			RADIOSONDES		
	Date	Time		Date	Time	
		(GMT)	(MST)		(GMT)	(MST)
7-8 August 1973						
				73/8/7	12	5
descending (day)	73/8/7*	17	10			
				73/8/8*	00	17
ascending (night)	73/8/8	4	21			
				73/8/8	12	5
9-10 August 1973						
				73/8/9	12	5
descending (day)	73/8/9*	17	10			
				73/8/10*	00	17
ascending (night)	73/8/10	4	21			
				73/8/10	12	5

* Used in this study.

Table 7.

temperature to determine if an inversion is present or not at satellite time. This information is available through the window channel radiance and a correction could be made, but for simplicity a more correct temperature profile was used since it was available for this study.

The radiosonde soundings used as initial guess profiles are listed in Table 8 along with data on position and elevation. For each of these radiosonde stations, VTPR radiance data at 17 GMT was used to derive the 3-dimensional temperature field around the radiosonde. The stations listed were considered to be mostly cloud free. If significant cloud coverage was detected the derived mesoscale temperature fields were usually scanty due to few clear column radiances. However, a very simple cloud correction was used which provided soundings down to an effective cloud top level (Shaw et al., 1970). This simple correction eliminated many problems caused by clouds and provided a significant increase in available soundings. More sophisticated cloud correction methods are being developed by Chahine (1974 & 1975) and further improvements in horizontal resolution will allow satellite sounders to better see between clouds (Stamm and Vonder Haar, 1970). But for this study, if clouds were detected they were considered as contaminants, and the sounding below the effective cloud level was neglected due to the isothermal tendency of the retrieved sounding below the clouds (Jastrow and Halem, 1973). Variations in surface elevation have an effect similar to clouds but these variations were also accounted for in the variable surface pressure in the same way as clouds.

Up to 35 clear-column soundings in an array of 7 scan lines of 5 spots each were derived around each of the initial guess radiosonde soundings. The position of the radiosonde-satellite mesoscale

RADIOSONDE STATIONS

8 August 1973 00 GMT

Station	Abbre-viation	WMO No.	Latitude ($^{\circ}$N)	Longitude ($^{\circ}$W)	Longitude ($^{\circ}$E)	Elevation (meters)	Elevation (mb)
Lander, WY	LND	72576	42.8	108.7	251.3	1700.	826.
Rapid City, SD	RAP	72662	44.0	103.1	256.9	966.	897.
Huron, SD	HON	72654	44.4	98.2	261.8	393.	960.

10 August 1973 00 GMT

Station	Abbre-viation	WMO No.	Latitude ($^{\circ}$N)	Longitude ($^{\circ}$W)	Longitude ($^{\circ}$E)	Elevation (meters)	Elevation (mb)
Glasgow, MT	GGW	72768	48.2	106.6	253.4	700.	933.
Lander, WY	LND	72576	42.8	108.7	251.3	1700.	830.
Bismarck, ND	BIS	72764	46.8	100.8	259.2	506.	954.
Rapid City, SD	RAP	72662	44.0	103.1	256.9	966.	905.
Huron, SD	HON	72654	44.4	98.2	261.8	393.	966
North Platte, NE	LBF	72562	41.1	100.7	259.3	849.	917.
Denver, CO	DEN	72469	39.8	104.9	255.1	1616.	839.
Dodge City, KS	DDC	72451	37.8	100.0	260.0	790.	922.

Table 8.

temperature fields derived for each initial guess are outlined in Figure 12 and 13. These derived mesoscale fields are approximately 5° of latitude on a side, large enough to make a nearly continuous sounding field over the Northern Great Plains region as was done to display the satellite soundings for comparison with synoptic analyses from radiosonde soundings alone. By looking at the overlap between these mesoscale fields, relative bias errors in the individual sounding fields can be detected and the relative accuracy of retrieved temperatures can be determined, but only by eliminating these biases does the true quality of satellite soundings become apparent.
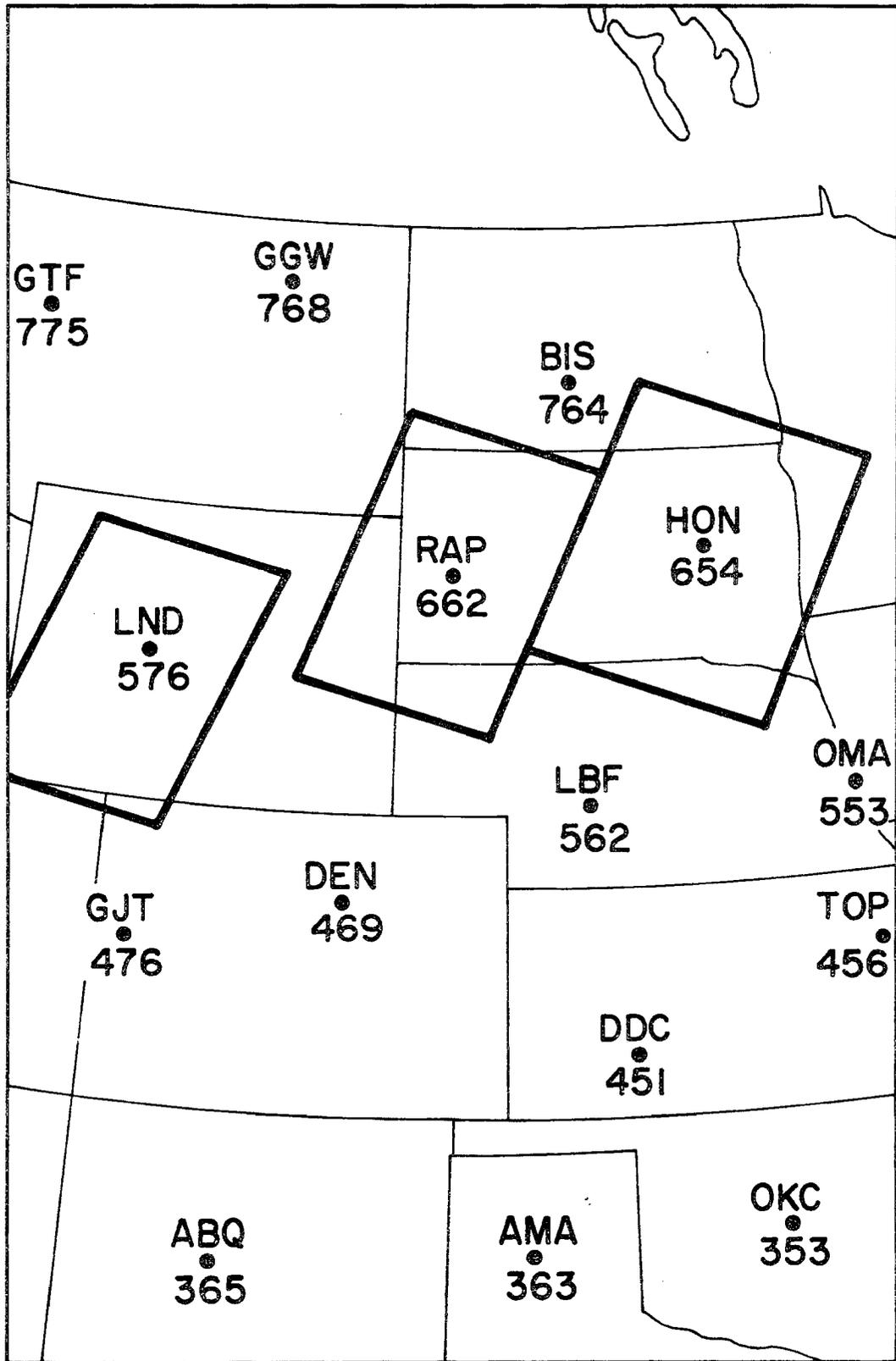
Figure 12.   Radiosonde-Satellite Mesoscale Fields
7 August 1973 17 GMT

GTF
775

GGW
768

BIS
764

HON
654

RAP
662

LND
576

OMA
553

LBF
562

DEN
469

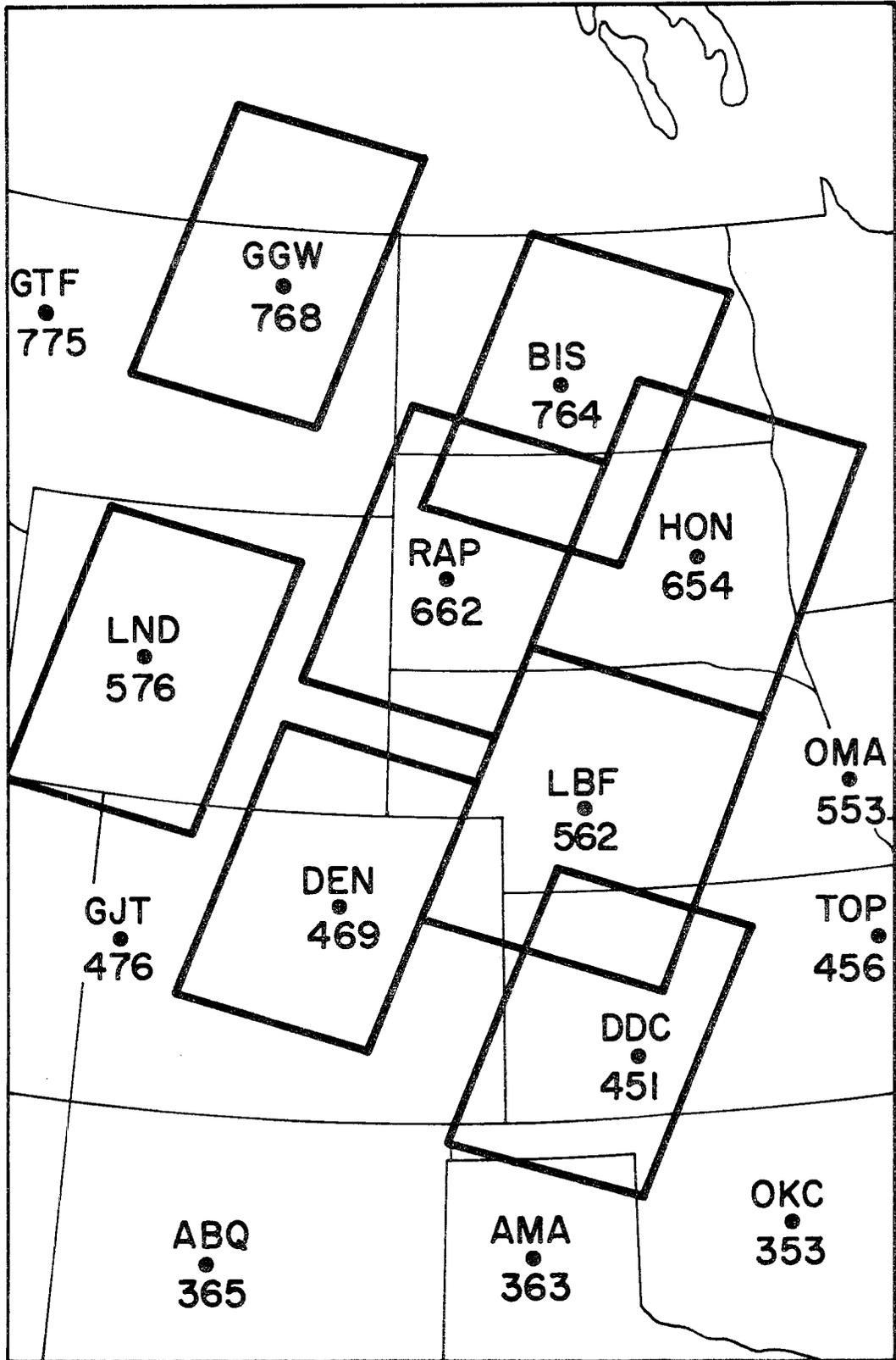GJT
476

TOP
456

DDC
451

ABQ
365

AMA
363

OKC
353

Figure 13. Radiosonde-Satellite Mesoscale Fields
9 August 1973 17 GMT

9.0 COMBINED MESOSCALE FIELDS; COMPARISON WITH SYNOPTIC ANALYSES

9.1 7 August 1973 17 GMT

The 500 mb pressure level was chosen to illustrate the results of the mesoscale temperature fields derived from combined use of satellite and radiosonde soundings. This level proved to be convenient to compare with 500 mb synoptic analyses made with conventional radiosonde soundings alone.

For each of the case study periods the individual mesoscale temperature fields were combined on one map for comparison with the synoptic analyses. To smooth the data slightly, thereby reducing the effect of random errors on the resultant temperatures, 4 to 6 temperatures were averaged to produce 9 temperatures in the mesoscale grid instead of the 35 original soundings at full resolution. These 9 temperatures from each mesoscale field were then combined as in Figure 14 for the first case study period 7 August 1973 at 17 GMT. However, in order to produce a combined temperature field which could be contoured across all the mesoscale fields the various biases between mesoscale fields had to be eliminated.

Because actual 17 GMT synoptic data is not available it is impossible to determine the actual temperatures which occurred at that time for comparison with the satellite-derived mesoscale temperature fields. Even when 17 GMT data was linearly interpolated between the standard 12 GMT and 00 GMT synoptic radiosonde sounding times the temperature biases were not necessarily correctly determined. The only other choice was to shift all the temperatures in each mesoscale field so that the contours were continuous at the overlapping areas or at the edges of the individual mesoscale temperature fields. The actual amount needed

-9

-10

-10.5

-9

-8

-8.57

-10

-10.3

-10.1

-9.3

-9.2

RAP

HON

-9.6

-9

-9.3

-9.2

-7.4

-9.1

LND

-9.5

-8.4

-8.3

-8

-8.2

-7.3

-8.3
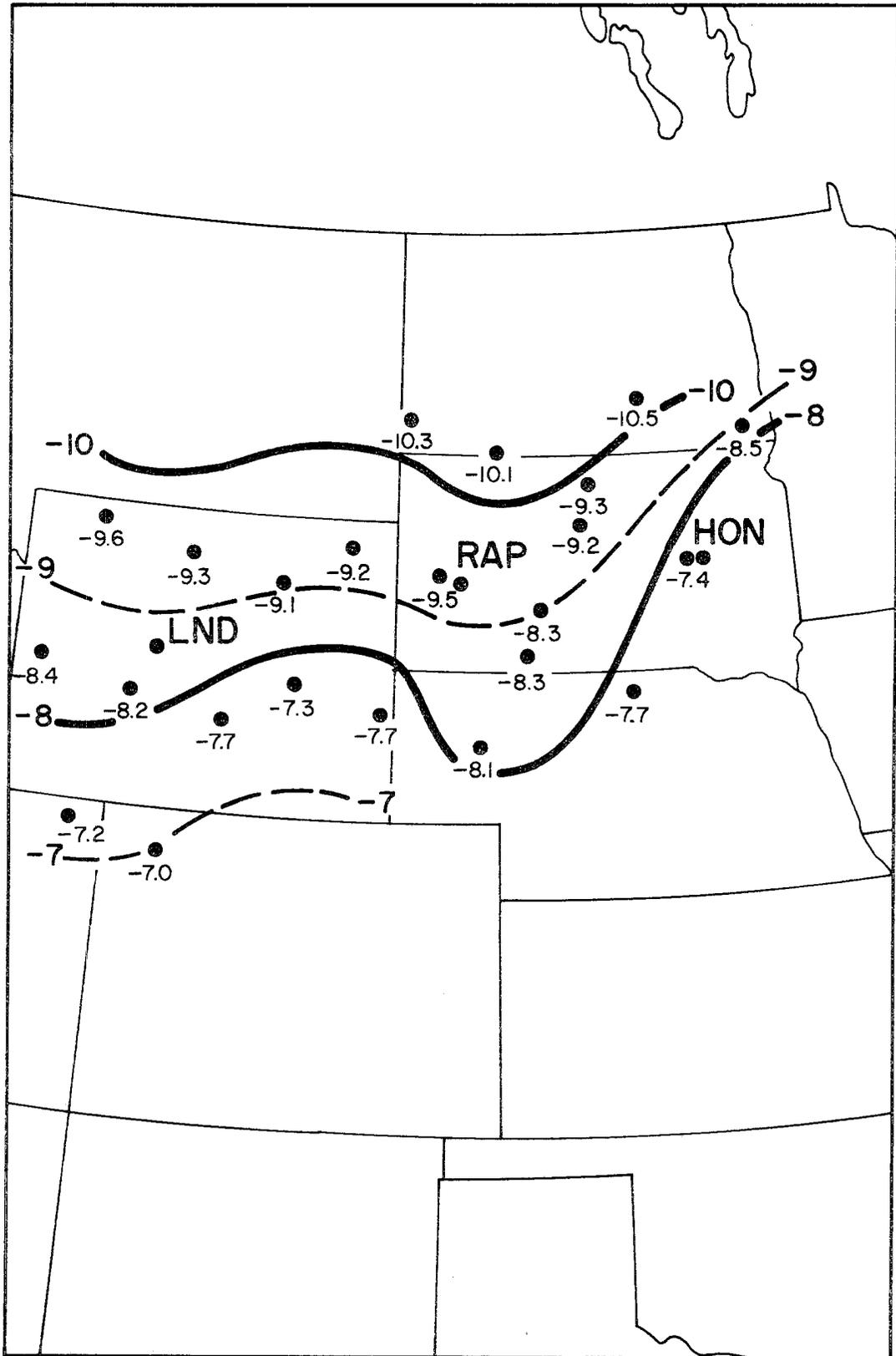
-7.7

-7.7

-7.7

-8.1

-7

-7.2

-7

-7.0

Figure 14. Combined 500 mb Mesoscale Temperatures (Celsius)
7 August 1973 17 GMT

to be added or subtracted from the temperature fields was calculated from the overlapping sounding pairs from different mesoscale fields. The only difference between the two overlapping soundings was the initial guess profile. The observed radiances used to derive the soundings by iteration were identical.

There existed a very high correlation between the derived temperature pairs in the overlap regions of adjacent mesoscale temperature fields which used different radiosonde soundings as initial guess. A relative bias between the fields could then easily be determined. In a case where the mesoscale fields did not overlap, as for the fields around Lander and Rapid City on 7 August 1973, the relative bias could still be determined fairly easily for adjacent pairs of retrieved temperatures.

The relative bias was $+2^{o}C$ for the Huron mesoscale field compared to the adjacent Rapid City mesoscale field. The Lander and Rapid City fields required no adjustment relative to each other. With the $2^{o}C$ bias subtracted from the derived temperatures around Huron, the combined fields were contoured as a continuous sounding network. The determination of relative biases was very useful in analyzing the individual mesoscale fields, however, the actual bias could not be determined without actual 17 GMT data which was unavailable. The combined mesoscale fields could still contain a positive or negative bias depending on which mesoscale field was assumed to be correct and the others were adjusted to match. On this first case study period the Lander mesoscale field near zero zenith angle was assumed to be correct and the temperature adjustment of $-2^{o}C$ was absorbed by the mesoscale field around Huron.

For a comparison the 7 August 1973 12 GMT and 8 August 1973 00 GMT 500 mb synoptic temperature analyses were drawn as well as a linearly-interpolated synoptic analysis at 17 GMT. These are shown in sequence in Figures 15, 16, and 17.

It appears that applying no correction to the Lander mesoscale field was a fairly good choice. The 17 GMT interpolated temperatures at Lander and Rapid City are only about $1^{\circ}C$ warmer than the temperatures from the mesoscale fields at those same locations. Both the Lander and Rapid City mesoscale fields could have been raised $1^{\circ}C$ and the Huron mesoscale temperatures lowered only $1^{\circ}C$.

The 12 GMT Huron radiosonde was missing which did not allow the calculation of a 17 GMT interpolated temperature for comparison, but from the 17 GMT interpolated field around Huron it appears that the satellite-derived temperatures around Huron may be at least $1^{\circ}C$ too warm. This may be due to the large zenith angle of the satellite radiances of about 30° around Huron. The correction for this large zenith angle may need adjustment as it seems that retrieved temperatures gradually increase with increasing zenith angle.

If no correction was made for increasing zenith angle the retrieved temperatures would be too low due to lower observed radiances. At larger zenith angles the longer atmospheric path would require a weighting function which would peak out at a higher and colder level in the atmosphere. The observed radiances would then be lower and the retrieved temperature profiles would appear colder. Therefore, the correction for zenith angle may be too large since retrieved temperatures appear to increase with increasing zenith angle.
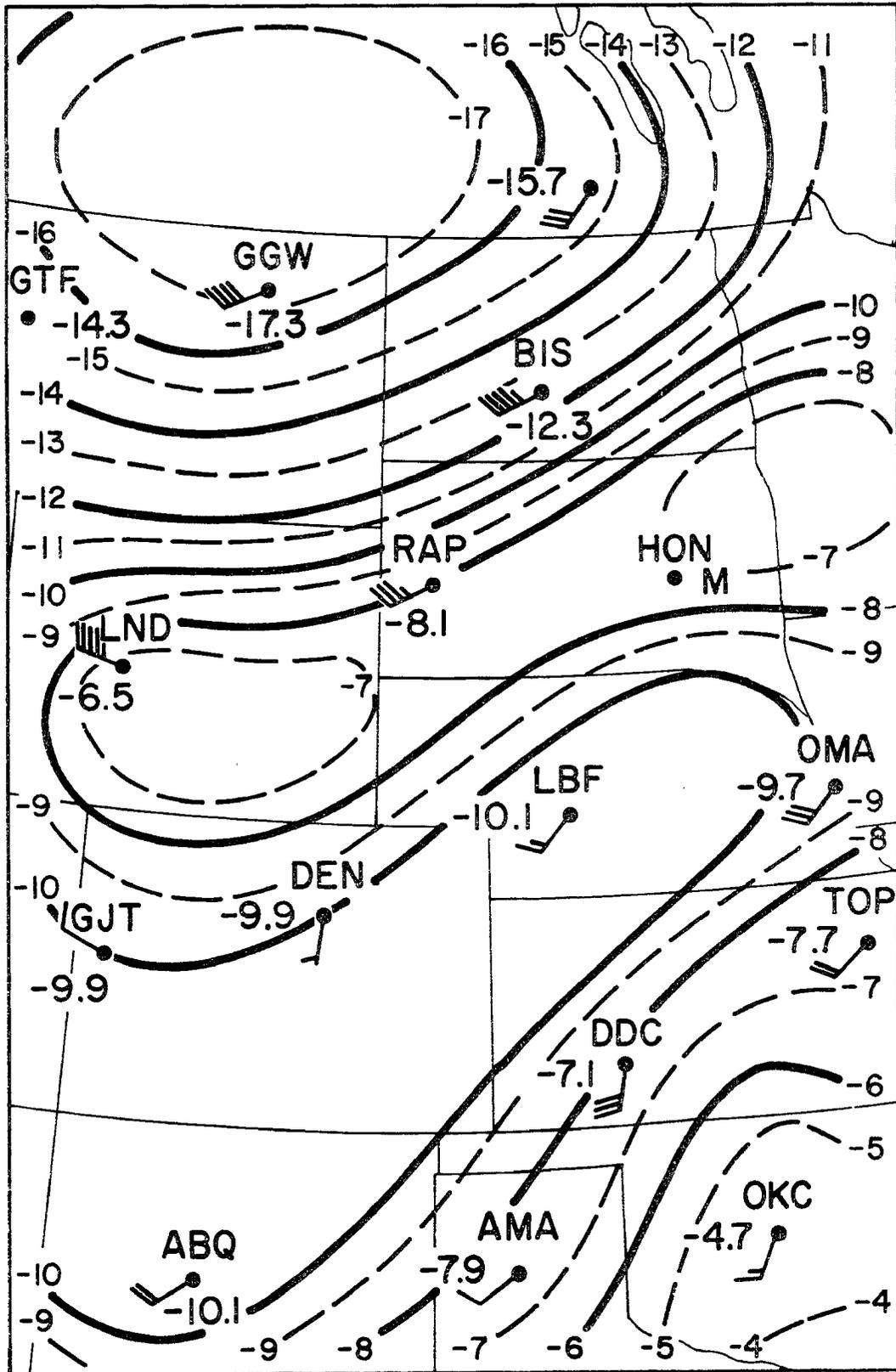
Figure 15.   500 mb Synoptic Analysis
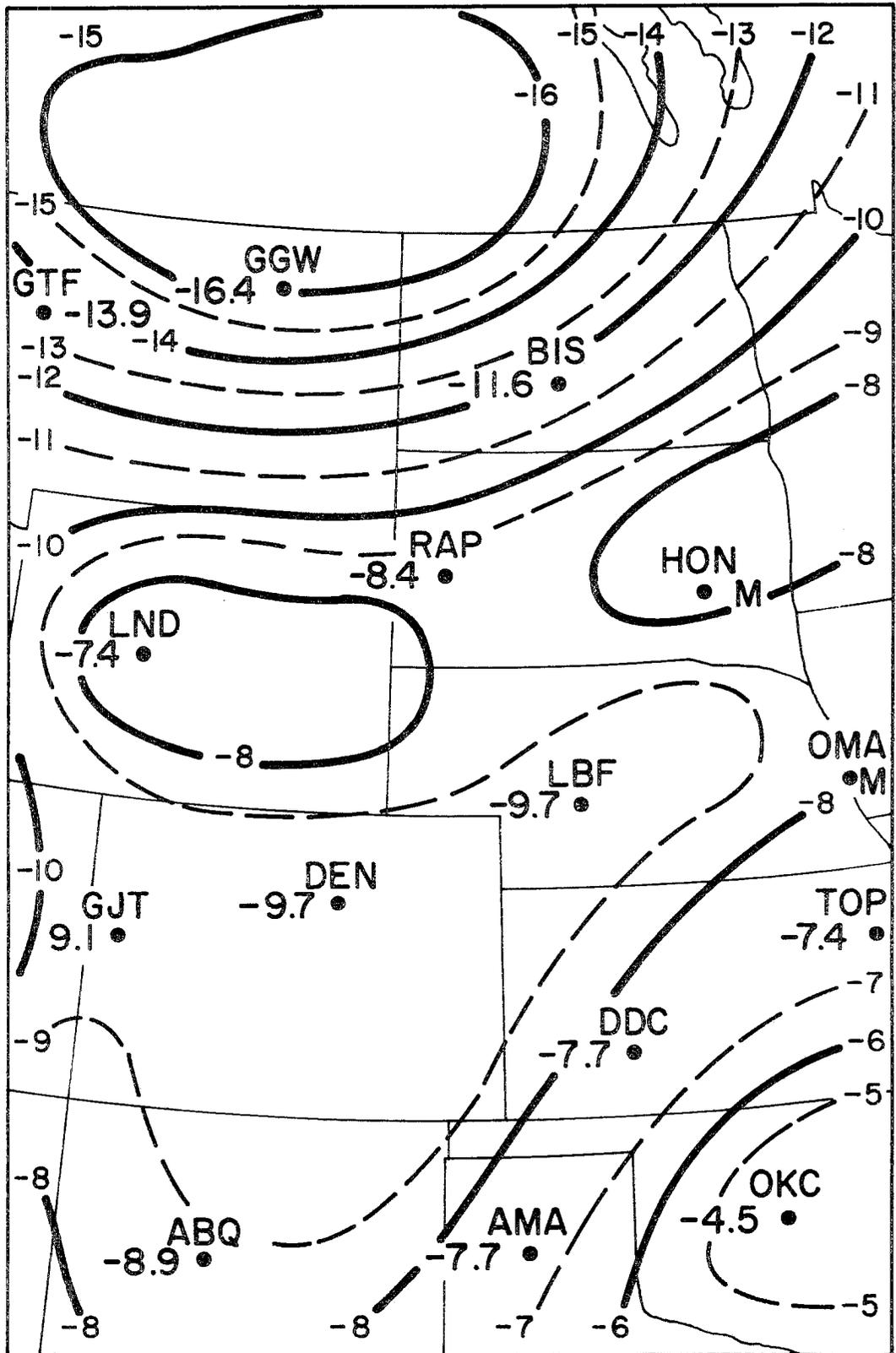7 August 1973 12 GMT
(Radiosonde Temperatures Alone)

Figure 16. 500 mb Synoptic Analysis
7 August 1973 17 GMT Interpolated
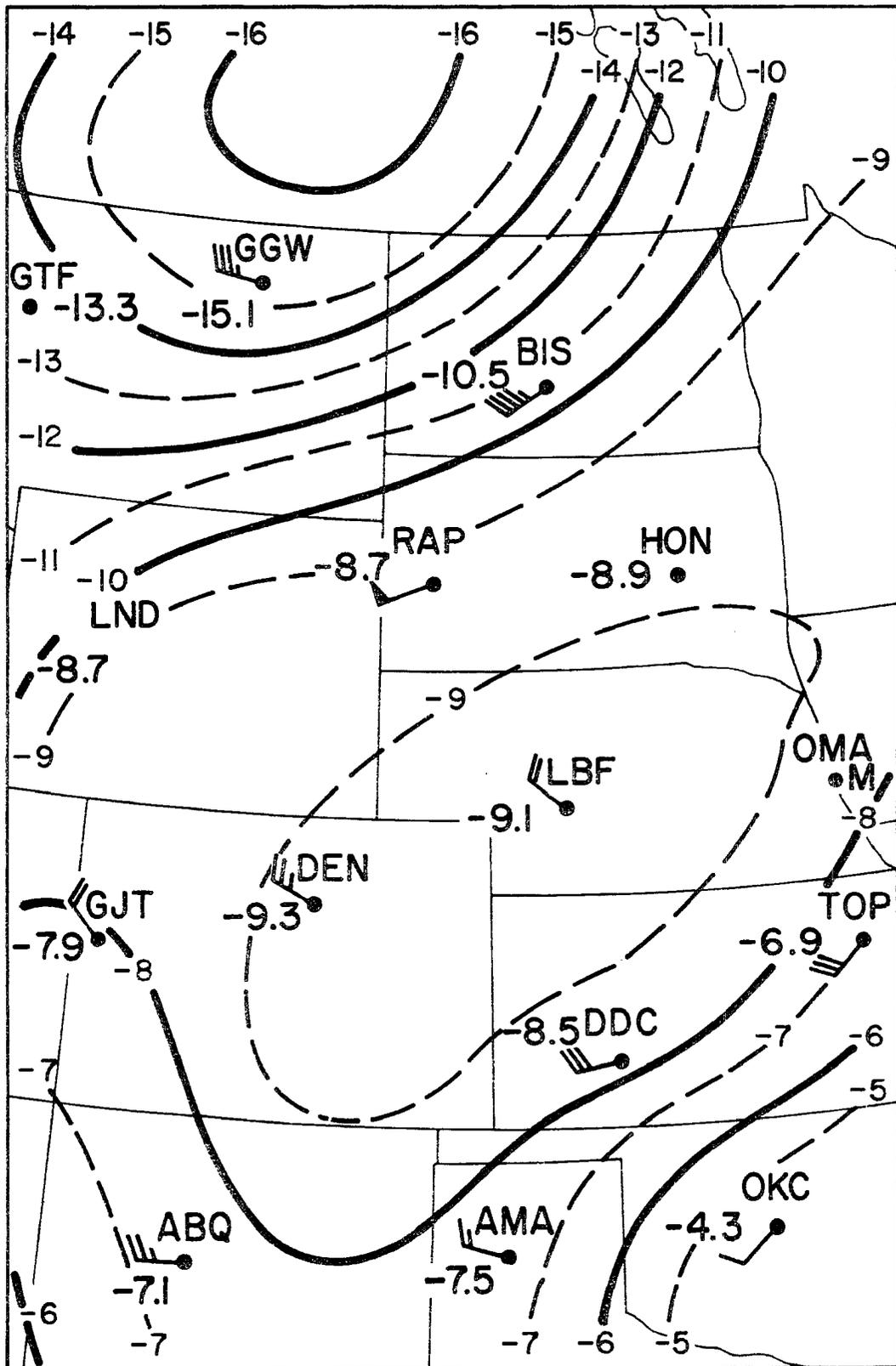(Radiosonde Temperatures Alone)

Figure 17. 500 mb Synoptic Analysis
8 August 1973 00 GMT
(Radiosonde Temperatures Alone)

One interesting feature of the combined mesoscale fields in Figure 14 is that the temperatures around Rapid City are lower than those around Lander or Huron. This feature is also apparent in the 12 and 17 GMT interpolated synoptic analyses in Figures 15 and 16. Apparently the combined mesoscale temperature field duplicates this feature which appears similar to a cold shortwave on the larger 500 mb cold trough. The ability to pick out this feature was dependent on the satellite observed radiances since the initial guess 500 mb temperatures used were the almost identical 00 GMT temperatures in Figure 17.

In a similar fashion the qualitative mesoscale moisture fields were combined in Figure 18. Again, the overlapping radiance difference pairs were used to determine relative biases between the mesoscale fields which arose mainly from different initial guess moisture profiles. Because the moisture information is of a qualitative nature in the form of a radiance difference between observed and calculated H_2O channel radiances (calculated minus observed), the choice of a "correct" mesoscale field is arbitrary. By using any mesoscale field as a basis a similar figure could be drawn with slightly different numbers. The adjustments, however, were on the order of 1 to 2 radiance units ($mW/m^2/sr/cm^{-1}$) in order to make the combined field continuous. Correlation between overlapping pairs of numbers was again very high.

These radiance differences as qualitative moisture indicators can only be used as such since no significant data base existed in this case to correlate these radiance differences with actual moisture values. There does, however, appear to be a significant change in moisture across portions of the combined mesoscale fields. A dry tongue east of Lander and passing through Rapid City and Huron is apparent.
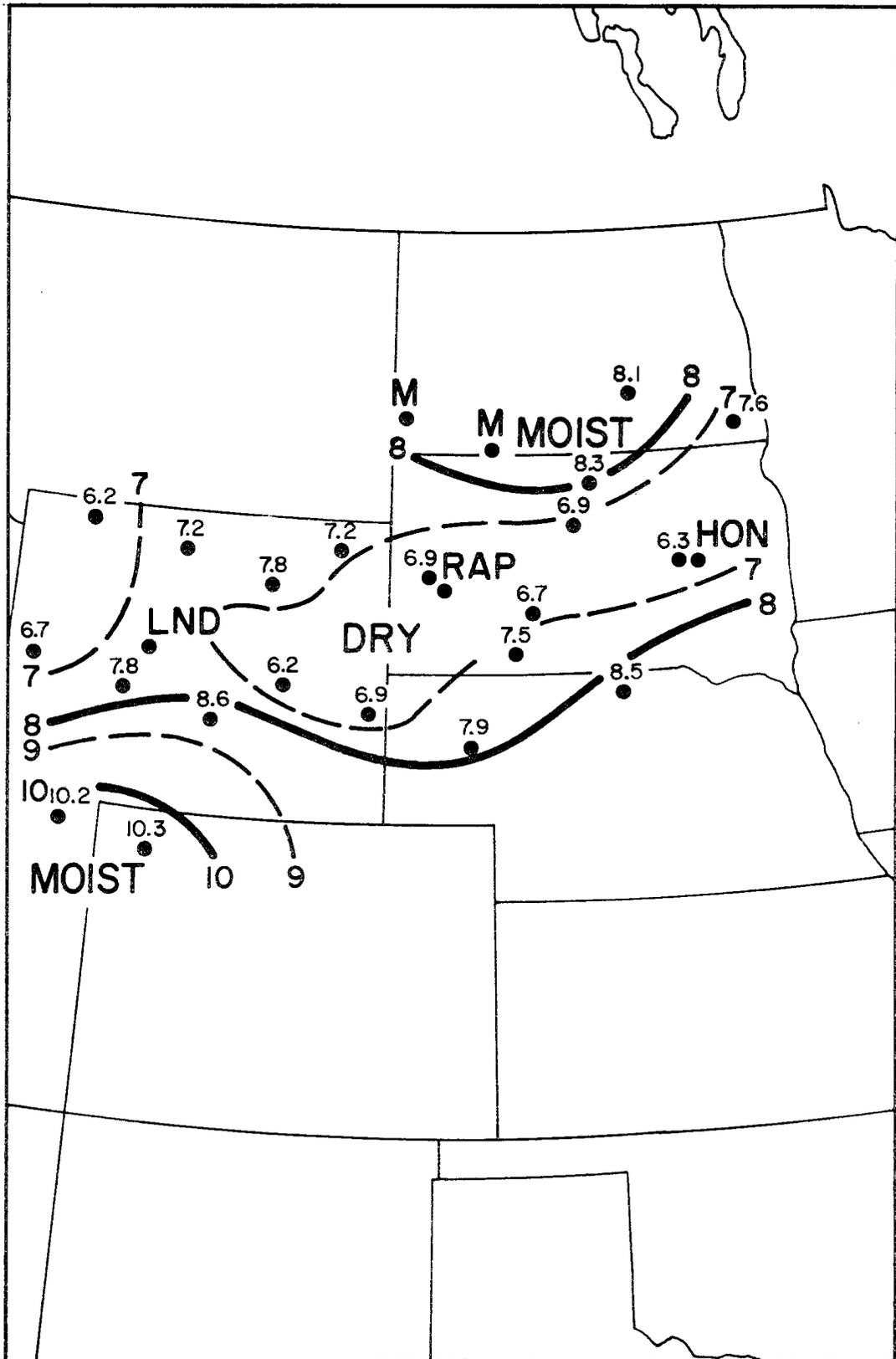
Figure 18. Combined Qualitative Vertically-Integrated
Moisture Values. 7 August 1973 17 GMT

According to the 500 mb synoptic temperature analysis at 12 and 17 GMT in Figures 15 and 16 this dry tonque seems plausible. A convergence zone at 500 mb over these same stations with resultant sinking motion, shows up as a warm region from Lander and extending to the east-northeast. This sinking and drying motion should also produce a relatively dry region or tongue in the same area, which is what is shown in the combined qualitative moisture fields.

The ATS-3 visible picture in Figure 19 at 21 GMT for this day, can be used to verify the above conclusions. The 21 GMT period was chosen as near the peak of convective activity for the day. The lack of convective activity along a line through Lander and Huron can be an indication of such convergence, subsidence, and drying of the atmosphere. Further to the north and south the presence of clouds rules out such strong subsidence. Moisture also appears to be more abundant to the north and south but this may be more a result of atmospheric motion, such as lack of subsidence or positive vertical motion, than it is a source of convective energy.

9.2 9 August 1973 17 GMT

For the second case study period, 9 August 1973 at 17 GMT a similar combination of 500 mb mesoscale temperature fields is shown in Figure 20. This set included 8 individual mesoscale fields rather than only 3 fields for the first case study period. The combined field was again produced by calculating relative biases between overlapping pairs of retrieved temperatures and adding or subtracting these biases to produce a continuous sounding network. The additive biases ranged from zero at southern stations to $-3^{o}C$ at Bismarck and were all negative due to the warmer 500 mb initial guess temperatures at 00 GMT than at the
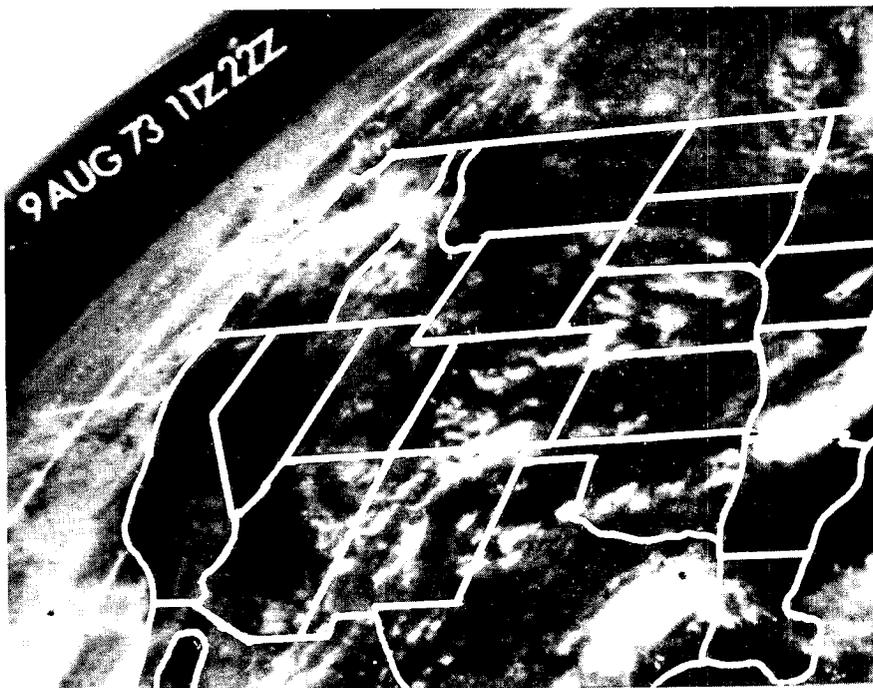
Figure 19. ATS-3 Visible Picture
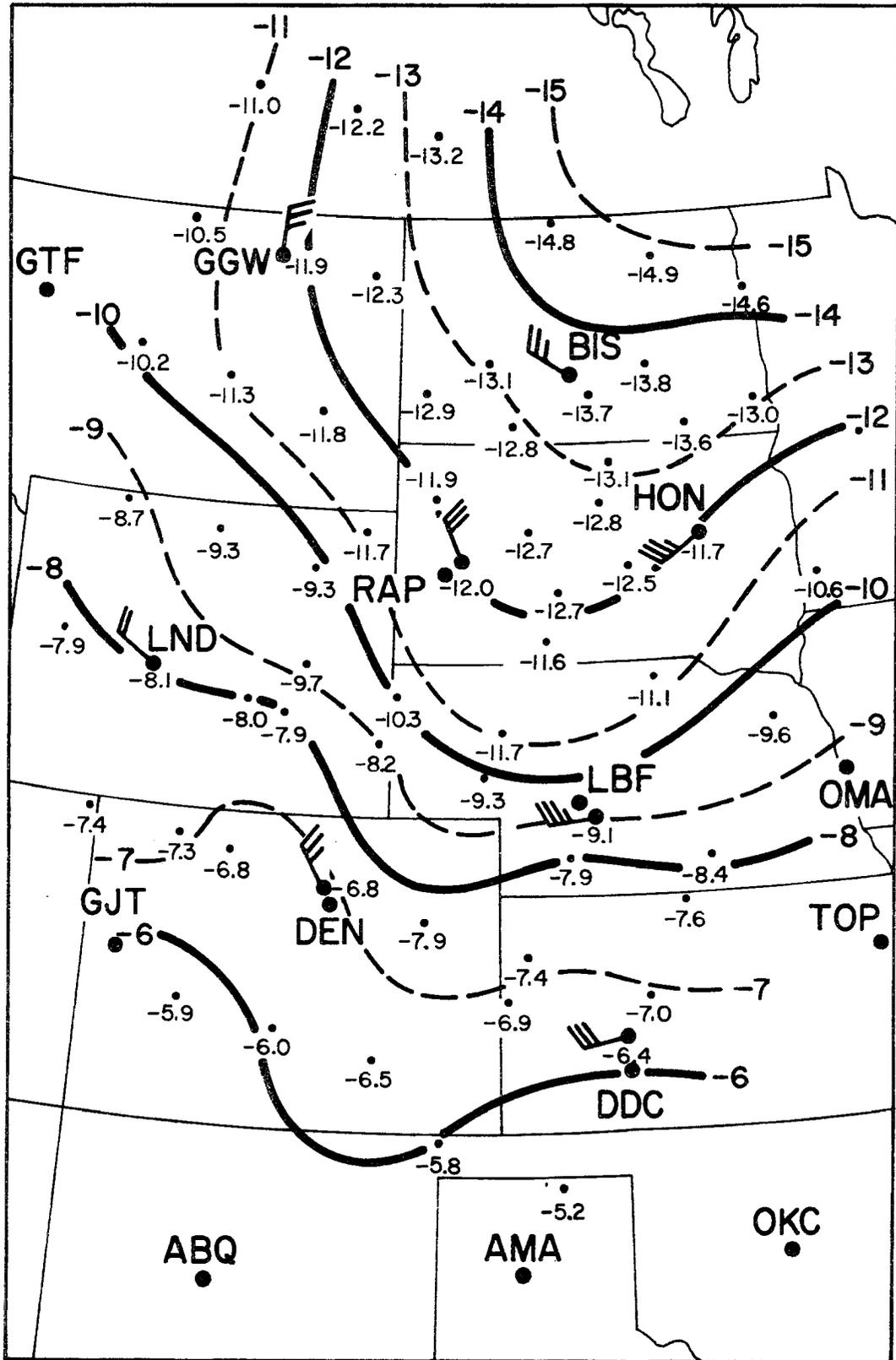7 and 9 August 1973 21 GMT (14 MST)

Figure 20. Combined 500 mb Mesoscale Temperatures (Celsius)
9 August 1973 17 GMT
Thermal Winds 300-700 mb (knots)

12 GMT synoptic period or at the 17 GMT interpolated period. These 500 mb synoptic and interpolated analyses are shown in sequence in Figures 21, 22 and 23 for comparison with the combined 500 mb meso-scale temperature field at 17 GMT.

By subtracting up to $3^{o}C$ at Bismarck, the combined mesoscale temperatures around Bismarck, Rapid City, Huron and Glasgow matched the coldest 12 GMT synoptic temperatures in Figure 21 almost exactly. The interpolated temperatures at 17 GMT are all higher than the 12 GMT temperatures, therefore the decrease of up to $3^{o}C$ at Bismarck may have been too much for these northern stations. However, the central and southern mesoscale fields around Lander, North Platte, Denver and Dodge City appear progressively too warm by up to $3^{o}C$ as the southern most extremeties are reached.

These bias corrections were calculated to create a continuous sounding field which matched at the overlapping edges of individual mesoscale fields. If instead of a $-3^{o}C$ correction at Bismarck, no correction were made then a $+3^{o}C$ bias correction would be required at some southern stations making the temperatures up to $6^{o}C$ too warm. In either case the temperature changes appear to be 3 to $4^{o}C$ too large across the north-south extent of the combined mesoscale field. This results in a temperature gradient about $1^{o}C$ per 3 degrees latitude too strong in the north south direction. This excessive temperature grad-ient shows up well when the individual mesoscale fields are placed end to end and the individual temperature changes are added together to make a continuous sounding field over a 12 degree north-south latitude extent.
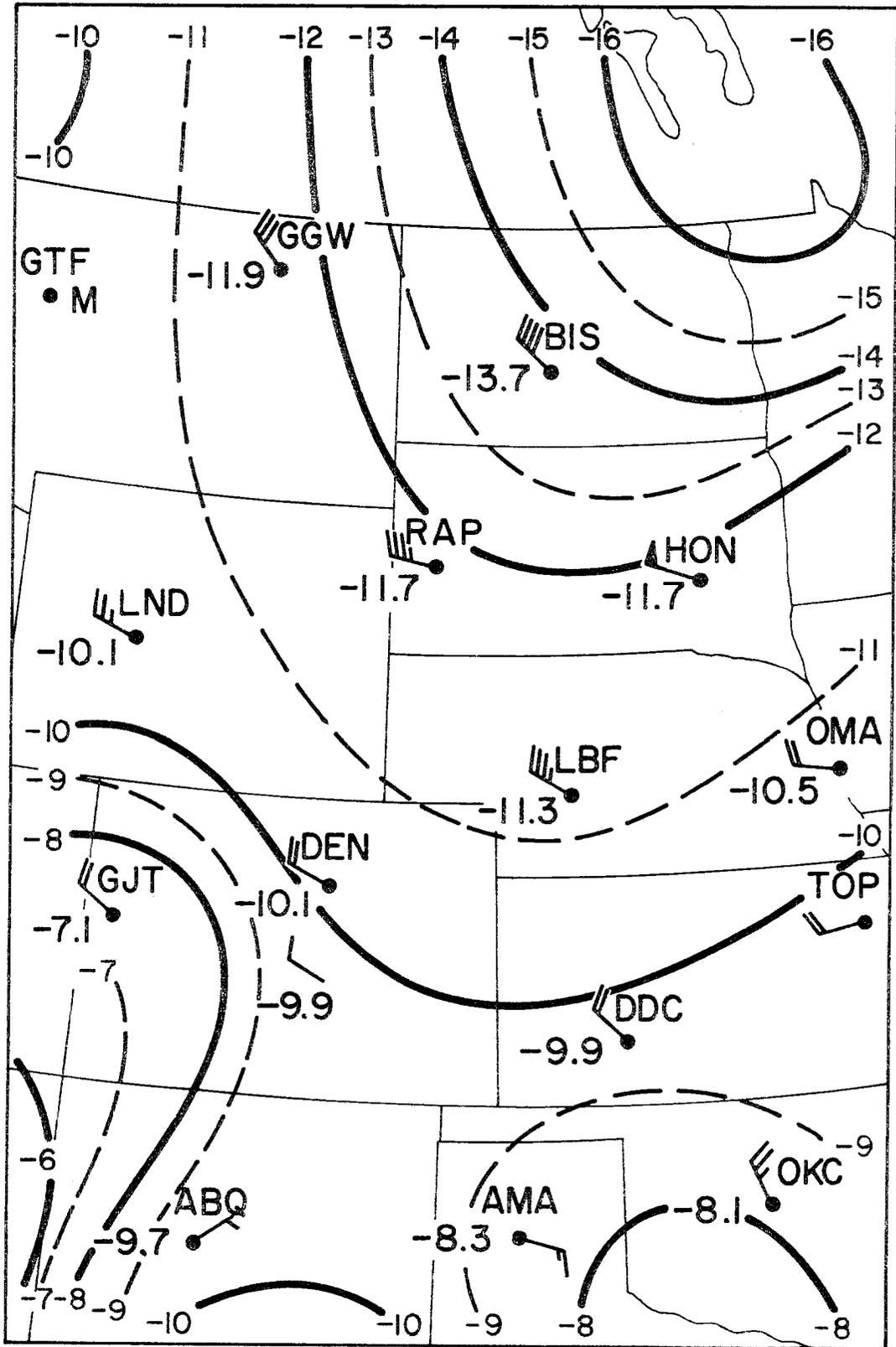
Figure 21. 500 mb Synoptic Analysis
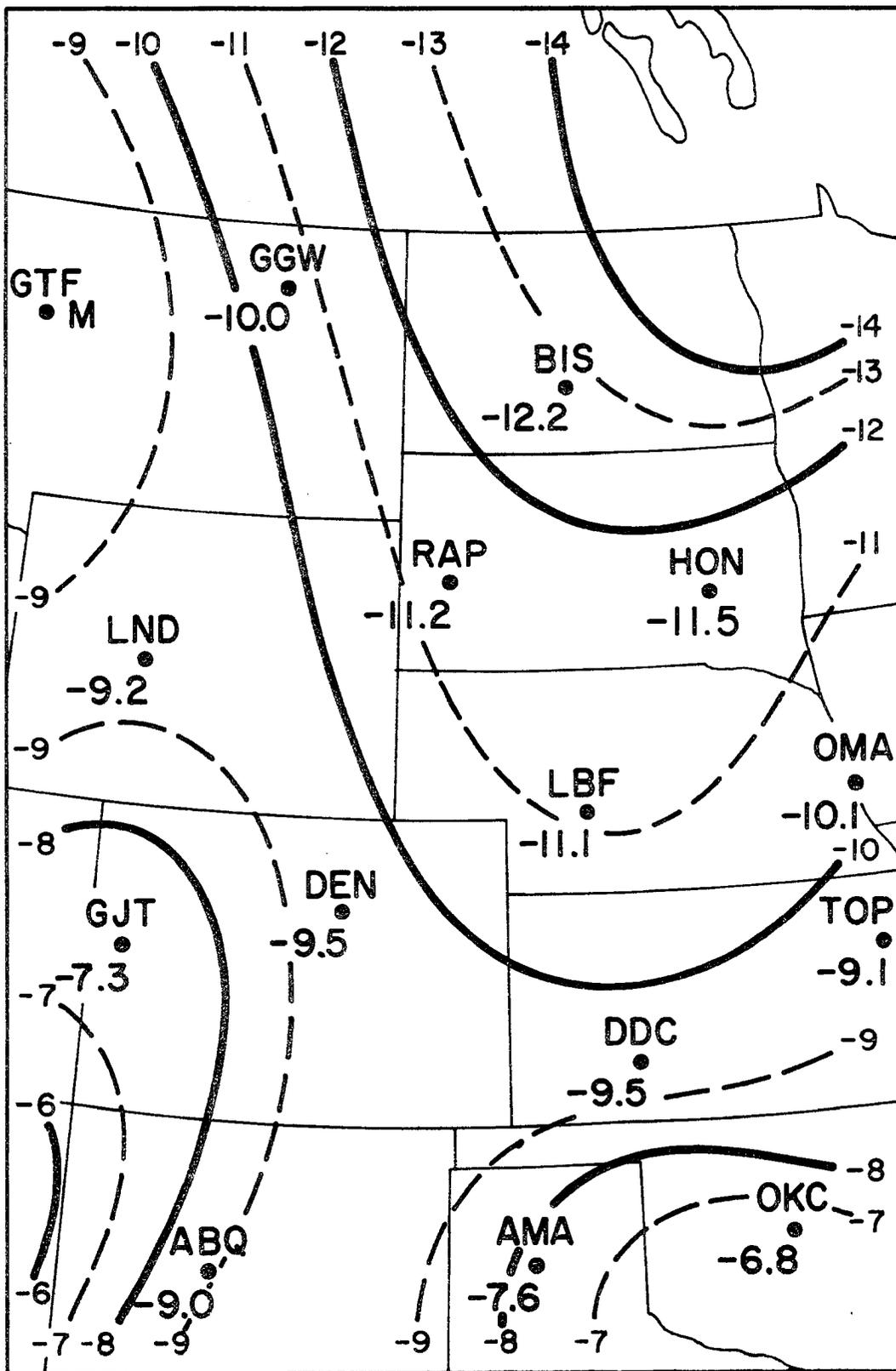9 August 1973 12 GMT
(Radiosonde Temperatures Alone)

Figure 22.   500 mb Synoptic Analysis
9 August 1973 17 GMT Interpolated
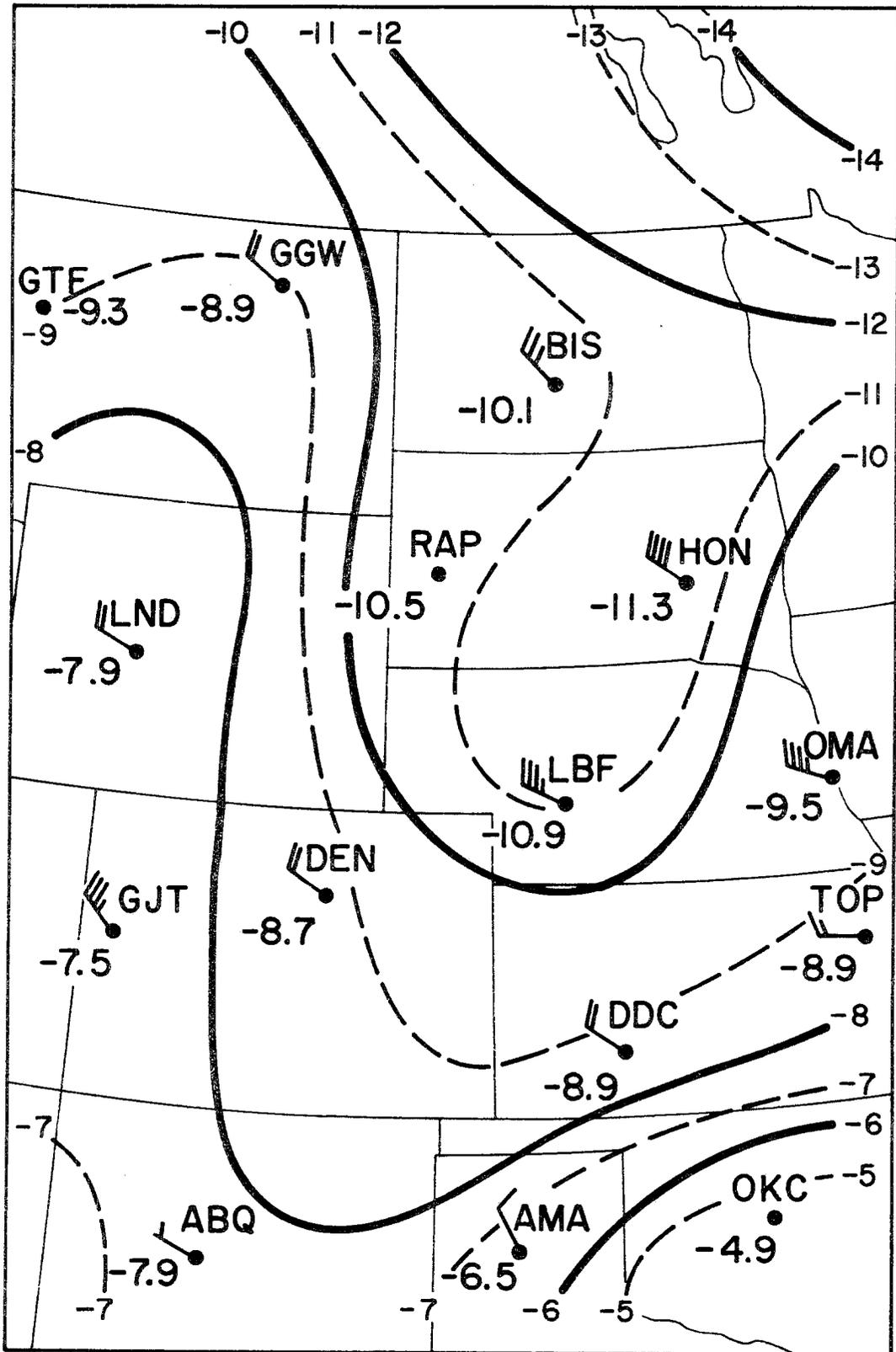(Radiosonde Temperatures Alone)

Figure 23. 500 mb Synoptic Analysis
10 August 1973 00 GMT
(Radiosonde Temperatures Alone)

The reason for the temperature gradient being too strong may be due to the use of the same radiosonde sounding as initial guess profile for all the retrieval soundings in a mesoscale grid. As one moves away from the original radiosonde sounding position near the center of each mesoscale field the radiosonde sounding becomes a progressively worse initial guess profile. With the same initial guess profile and therefore the same transmittances across the whole mesoscale field, changes in radiances must be accompanied by stronger changes in the retrieved temperature profiles than if the initial guess or transmittances were also allowed to change.

Other than the temperature gradients being too strong the temperature contours in the 17 GMT combined mesoscale fields appear to agree very well with the 12 GMT synoptic and 17 GMT interpolated synoptic analyses in Figures 21 and 22. It should also be noted that by averaging from 4 to 6 individual retrieved temperatures to produce only 9 temperatures in each mesoscale field that the random noise in the mesoscale temperatures was reduced from about $\pm 1^{\circ}C$ to less than $\pm .5^{\circ}C$. In spite of this, there still appears to be more fine structure than in the synoptic analyses. The cold trough axis in the 17 GMT combined field is located more nearly like the cold trough axis at 12 GMT than at 17 GMT or at 00 GMT even though 00 GMT temperatures were used as initial guesses. This may mean that the 17 GMT interpolated analysis should look more like the 12 GMT analysis in terms of cold trough position and/or colder temperatures.

Thermal winds between 300 and 700 mb, vertical change in geostrophic winds (Holton, 1972), were calculated for each of the individual mesoscale temperature fields and are also shown in Figure 20. These values

range from 20 to 35 knots and may be a little too strong especially near Huron and North Platte where the horizontal temperature gradients also appear a little too strong. This is just another indication of the strength of these temperature gradients if winds can be assumed to be geostrophic at these levels.

The moisture analysis for this second case study period is shown in Figure 24. Instead of qualitative moisture values in terms of differences between calculated and observed radiances, this is a plot of precipitable water values at 17 GMT. To plot actual moisture variables instead of radiance differences a correlation was found between the bias-adjusted radiance differences at 17 GMT and two different interpolated moisture variables at 17 GMT. One of these variables with the highest correlation to the qualitative radiance differences, the H_2O mixing ratio at 700 mb, is plotted in Figure 25. The 700 mb level is just below the mean peak level for the H_2O channel weighting function which varies with the moisture content of the atmosphere. Only 8 pairs of points for the 8 radiosonde stations were available, but a correlation of .95 existed between them.

The other moisture variable, the vertically-integrated precipitable water, is plotted against radiance difference in Figure 26. The correlation between 17 GMT interpolated precipitable water values and the 17 GMT adjusted radiance differences was less at .87 than those for 700 mb mixing ratio, but precipitable water is probably a more widely used moisture variable than the mixing ratio at one level alone. So, from these 8 data pairs and the fairly strong correlation between them, a linear least-squares line was fit to the points in Figures 25 and 26.
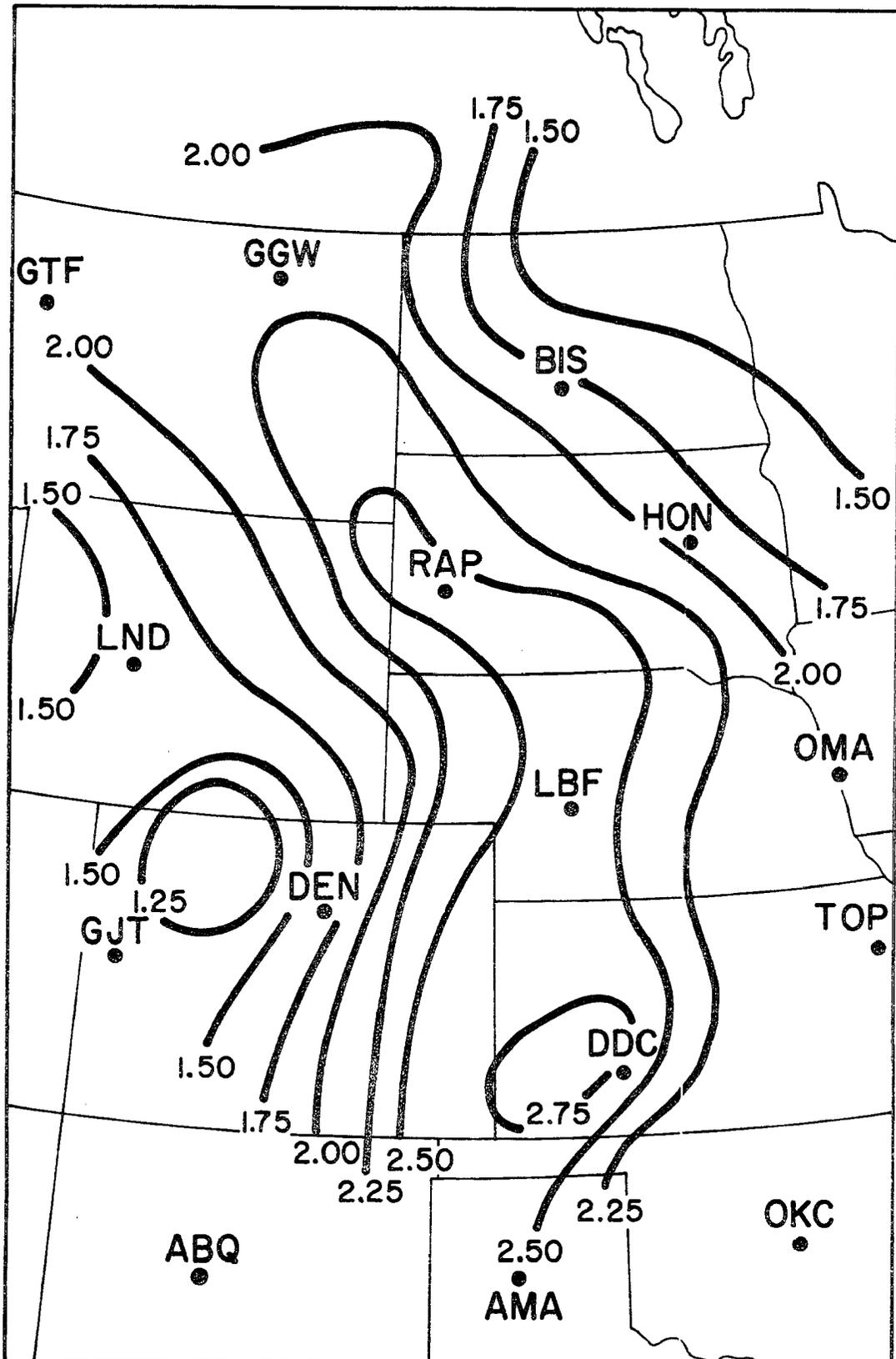
Figure 24. Combined Mesoscale Precipitable Water Fields (centimeters)
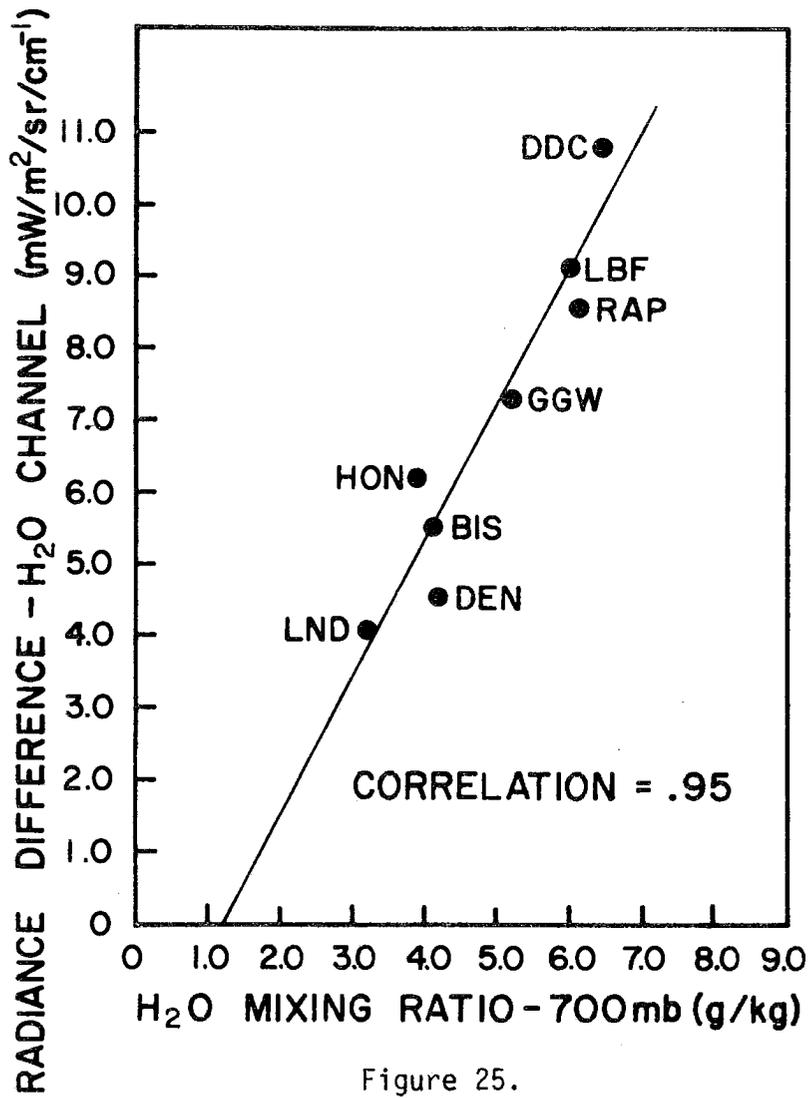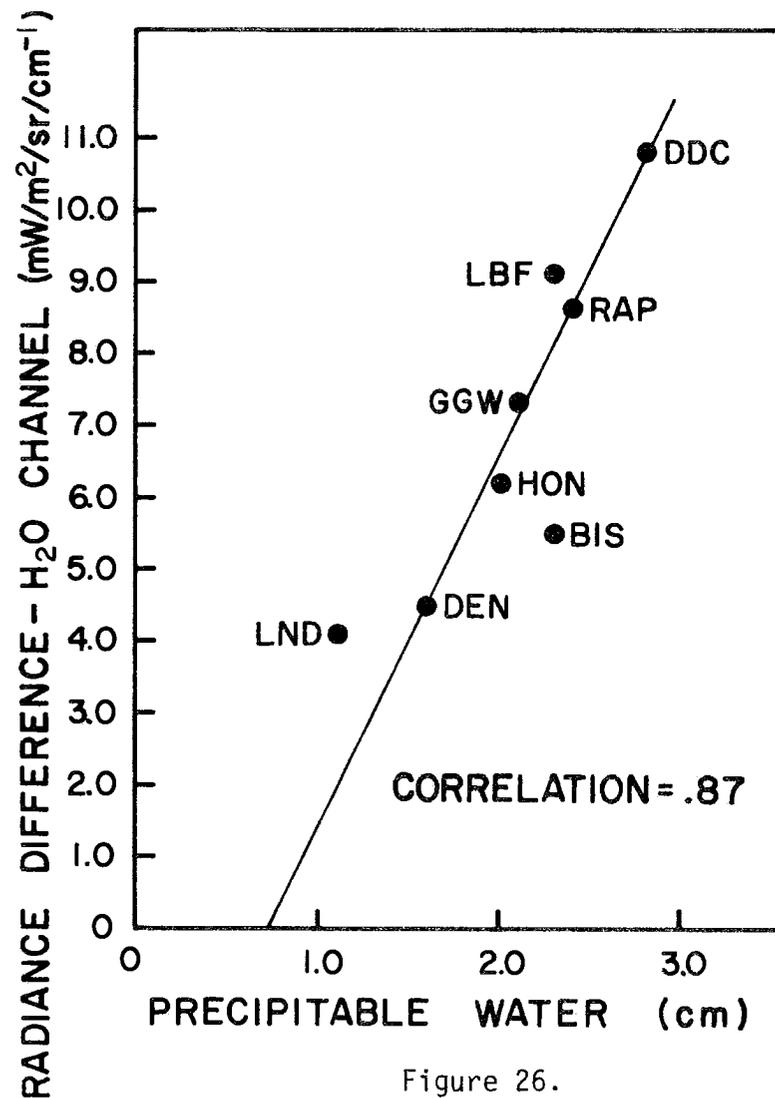9 August 1973 17 GMT

Figure 25.

Figure 26.

9 August 1973 17 GMT

Using this correlation line for precipitable water, the radiance differences were converted into equivalent precipitable water values which were plotted and contoured.

The precipitable water values used at 17 GMT are interpolated values and the actual precipitable water values may be higher or lower, but since the correlation is a strong one, the results are fairly reliable. Interpolated precipitable water values at various stations vary by less than .5 cm from the linear correlation line in Figure 26. This is the error associated with each precipitable water contour in Figure 24.

The moist tongue from Dodge City up through North Platte and Rapid City is above the noise level of .5 cm. Low values of precipitable water around Bismarck and west of Denver are probably false readings. Clouds near Bismarck and the mountains west of Denver produced especially low precipitable water values. The cloud and surface elevation correction technique raised the surface up to almost 700 mb in some cases which resulted in low calculated H_2O radiances and, therefore, low radiance differences which converted into low precipitable water values.

The ATS-3 Visible Picture for 9 August 1973 at 21 GMT in Figure 19 shows the weather situation later in the day. The moist tongue in western South Dakota, western Nebraska and western Oklahoma, when coupled with the leading edge of the 500 mb cold trough, should be a prime suspect area for convective activity. Some of this convection is apparent in western Nebraska and northeastern Colorado and is probably associated with a dry line through eastern Wyoming. Also, suppressed convective activity takes place around Dodge City probably due to

warmer upper level temperatures and reduced surface temperatures possibly due to clouds in this area earlier in the day.

If these combined 500 mb temperature and precipitable water fields were used along with some surface observations near 17 GMT the suspect areas for convective activity could most likely be chosen with reasonable accuracy. No surface observations were used in this study, only the results of remote temperature soundings were presented. It is a matter of applying this improved satellite-plus-radiosonde data base to the problem of analysis or forecasting which still remains.

10.0 SUMMARY AND CONCLUSIONS

The usefulness of VTPR or similar ITPR sounding radiances in data sparse regions such as over the oceans has been demonstrated by many studies. However, the use of similar sounding radiances over land areas is less common. Land areas present special remote sounding problems but they also offer the possibility of using radiosonde soundings as best initial guess profiles. The radiosonde sounding also enables corrections to be made to the retrieved temperature profiles if biases occur due to radiances or transmittance calculations. The radiosonde, therefore, provides an anchor upon which the mesoscale field around the radiosonde sounding can be tied and the retrieved temperatures fill out the branches on this tree.

It is very helpful to have a radiosonde launch coincident in time with the satellite pass in order to apply the desired corrections accurately. If no such launch is available, two radiosonde soundings which provide adjacent mesoscale fields could be used. By looking at the overlap between individual mesoscale sounding fields, relative biases can be determined and appropriate corrections made. However, some absolute bias may still exist in the combined fields unless some actual temperature values at satellite time existed for comparison.

The individual mesoscale temperature fields at full resolution provide soundings every $(70 \text{ km})^2$ for VTPR. However, if some resolution can be sacrificed, the data quality can be improved. Random errors of $\pm 1^\circ C$ can be reduced to less than $\pm .5^\circ C$ by averaging 4 to 6 temperatures, thereby reducing resolution by a factor of 4. Combining such mesoscale temperature fields on a common map can then provide an easy way of

comparing the combined radiosonde-satellite mesoscale temperature field to synoptic analyses provided by conventional radiosondes alone.

The contours on such a combined field appear to agree very well with synoptic analyses but the magnitude of the temperature gradient is too strong by about $1^{\circ}C$ per 3° latitude in one on the cases presented. In spite of these problems, it is obvious that the combined use of radiosonde and satellite soundings provides a product which is better than either system alone.

The combined data coverage and resolution far surpasses interpolation between conventional radiosonde soundings. Cold temperature troughs can be better located and fine structure between radiosonde soundings can be seen. Moisture information is also available in the form of differences between calculated and observed radiances or in the form of precipitable water content when this radiance difference can be calibrated. This requires at least a small sample of coincident radiosonde soundings and satellite water vapor channel radiance measurements. Again, in order to eliminate absolute biases, these measurements must be coincident in space and time, otherwise only a correlation relative to the moisture soundings used can exist between moisture and radiance differences.

The advantage of the added data coverage and resolution is especially apparent on the mesoscale where the conventional radiosonde soundings network is of little use. Even if radiosonde soundings are taken on a smaller mesoscale network the results can be combined with satellite sounding radiances to produce an even higher sounding resolution or at least a redundant set of satellite and radiosonde soundings. In many cases fewer radiosonde soundings can be used in a mesoscale

network while satellite sounding radiances fill in the gaps between the radiosonde soundings much as was done in this study to fill in between radiosonde soundings on the synoptic scale when the individual mesoscale fields were combined.

The ability to better locate low temperature troughs and temperature short waves in the upper atmosphere is of great value. These small forcing mechanisms are apparent only at higher resolution than is available with the conventional radiosonde sounding network alone. Moisture information on the mesoscale can also be indicative of the atmospheric motions such as convergence and downward vertical motion with drying effects. The amount of moisture is also a factor in the extent to which cumulus convective activity could take place in terms of moisture being an energy source for convection. Therefore, moisture, which in general varies rapidly on the mesoscale (Wark, 1974), is a predictor as well as a result of atmospheric motions.

This data can be used for both analysis and forecasting in mesoscale experiments. Even if not used in this mode the high resolution soundings may be useful in testing mesoscale numerical models which require data on a higher resolution than available with the conventional radiosonde network alone.

REFERENCES

Chahine, M.T., 1968: Determination of the temperature profile in an atmosphere from its outgoing radiance. Journal Optical Society of America, 58, 12, December.

Chahine, M.T., 1970: Inverse problems in radiative transfer: Determination of atmospheric parameters. Journal Atmo. Sci., 27, September.

Chahine, M.T., 1974: Remote sounding of cloudy atmospheres. I. The single cloud layer. Journal Atmo. Sci, 31, January.

Chahine, M.T., 1975: An analytical transformation for remote sensing of clear-column atmospheric temperature profiles. Journal Atmo. Sci., 32, October.

Duncan, L.D., 1974a: An Iterative Inversion of the Radiative Transfer Equation for Temperature Profiles. Atmospheric Sciences Lab, US Army Electronics Command, WSMR, Research and Development Tech. Report, ECOM-5534, March.

Duncan, L.D., 1974b: Approximations in Inverting the Radiative Transfer Equation. Atmospheric Sciences Lab, US Army Electronics Command, WSMR, Research and Development Tech. Report, ECOM-5534, July.

Duncan, L.D., 1975: Personal communication, H_2O transmittances derived via method used at NOAA-NESS for operational VTPR in data sparse regions.

Dyck, H.M., Jr., 1975: Test and Evaluation of a VTPR Retrieval System from Clear-Column NOAA-2 Radiances. Naval Postgraduate School, March.

Fritz, S., D.Q. Wark, H.E. Fleming, W.L. Smith, H. Jacobowitz, D.T. Hilleary and J.C. Alishouse, 1972: Temperature Sounding from Satellites. NOAA Tech. Report, NESS 59, July.

Hall, F.F., 1974: Infrared Transmission Spectrum. Handout in AT-761 Special Methods - Atmospheric Measurements, class taught at CSU.

Holton, J.R., 1972: An Introduction to Dynamic Meteorology. Academic Press, New York.

Jastrow, R. and M. Halem, 1973: Accuracy and coverage of temperature data derived from the IR radiometer on the NOAA-2 satellite. Journ. Atmo. Sci., 30, July.

Kaplan, L.D., 1959: Inference of atmospheric structure from remote radiation measurements. J. Optical Society of America, 49, 10.

Landsberg, H., 1966: Physical Climatology, Second Edition, Gray Printing Company, Inc., 1966.

McMillin, L.M., D.Q. Wark, J.M. Siomkajlo, P.G. Abel, A. Werbowetzki, L.A. Lauritson, J.A. Pritchard, D.S. Crosby, H.M. Woolf, R.C. Luebbe, M.P. Weinreb, H.E. Fleming, F.E. Bittner and C.M. Hayden, 1973: Satellite Infrared Soundings from NOAA Spacecraft. NOAA Tech. Report, NESS 65, September.

Shaw, J.H., M.T. Chahine, C.B. Farmer, L.D. Kaplan, R.A. McClatchey and P.W. Schaper, 1970: Atmospheric and surface properties from spectral radiance observations in the 4.3 micron region. Journ. Atmo. Sci., 27, August.

Smith, W.L., 1969: A Polynomial Representation of Carbon Dioxide and Water Vapor Transmission, ESSA Tech. Report, NESC 47, February.

Smith, W.L., 1972: Satellite techniques for observing the temperature structure of the atmosphere. Bulletin AMS, 53, 11.

Smith, W.L., H.B. Howill, J.C. Fisher, M.C. Chalfant and D.T. Hilleary, 1972: The infrared temperature profile radiometer (ITPR) experiment. The Nimbus-5 User's Guide, Goddard Space Flight Center, NASA, November.

Smith, W.L., H.M. Woolf, P.G. Abel, C.M. Hayden, M. Chalfant and N. Grady, 1974: Nimbus-5 Sounder Data Processing System, Part I. NOAA Tech. Memorandum, NESS 57, July.

Smith, W.L., H.M. Woolf, C.M. Hayden and W.C. Shen, 1975: Nimbus-5 Sounder Data Processing System, Part II. NOAA Tech. Memo., NESS 71, July.

Stamm, A.J. and T.H. Vonder Haar, 1970: A study of cloud distribution using reflected radiance measurements from the ATS satellites. Journ. Appl. Meteor., 9, June.

Suomi, V., T. Vonder Haar, R. Krauss and A. Stamm, 1971: Possibilities for sounding the atmosphere from a geosynchronous spacecraft. Space Research XI, Berlin.

U.S. Standard Atmosphere Supplements, 1966: Prepared under sponsorship of Environmental Science Services Administration, National Aeronautics and Space Administration, United States Air Force.

Wark, D.Q. and H.E. Fleming, 1966: Indirect measurements of atmospheric temperature profiles from satellites: 1. Monthly Weather Review, 94, June.

Wark, D.Q., 1974: Mesoscale Variations in Atmospheric Water Vapor in Tropical Regions Deduced from VTPR Measurements. Paper presented at IAMAP General Assembly, Melbourne.

Wark, D.Q., J.H. Lienesch and M.P. Weinreb, 1974: Satellite observations of atmospheric water vapor. Applied Optics, 13, 3, March.